

On finite volume effects in the chiral extrapolation of baryon masses

M.F.M. Lutz,¹ R. Bavontaweepanya,² C. Kobdaj,³ and K. Schwarz¹

¹*GSI Helmholtzzentrum für Schwerionenforschung GmbH,
Planckstraße 1, 64291 Darmstadt, Germany*

²*Mahidol University, Bangkok 10400, Thailand*

³*Suranaree University of Technology,
Nakhon Ratchasima, 30000, Thailand*

(Dated: July 28, 2014)

Abstract

We perform an analysis of the QCD lattice data on the baryon octet and decuplet masses based on the relativistic chiral Lagrangian. The baryon self energies are computed in a finite volume at next-to-next-to-next-to leading order (N³LO), where the dependence on the physical meson and baryon masses is kept. The number of free parameters is reduced significantly down to 12 by relying on large- N_c sum rules. Altogether we describe accurately more than 220 data points from six different lattice groups, BMW, PACS-CS, HSC, LHPC, QCDSF-UKQCD and NPLQCD. Values for all counter terms relevant at N³LO are predicted. In particular we extract a pion-nucleon sigma term of 39^{+2}_{-1} MeV and a strangeness sigma term of the nucleon of $\sigma_{sN} = 84^{+28}_{-4}$ MeV. The flavour SU(3) chiral limit of the baryon octet and decuplet masses is determined with (802 ± 4) MeV and (1103 ± 6) MeV. Detailed predictions for the baryon masses as currently evaluated by the ETM lattice QCD group are made.

INTRODUCTION

Various unquenched three-flavour simulations for the pion- and kaon-mass dependence of the baryon ground state masses are available [1–8]. Such data are expected to determine the low-energy constants of the three-flavour chiral Lagrangian formulated with the baryon octet and decuplet fields. A precise knowledge of the latter parameters is crucial for a profound understanding of meson-baryon scattering data based on coupled-channel dynamics as derived from the chiral Lagrangian (see e.g. [9–12]).

The chiral extrapolation of baryon masses with strangeness content is discussed extensively in the literature [13–30]. The convergence properties of a strict chiral expansion for the baryon masses with three light flavours are very poor, if existing at all for physical strange quark masses. Different strategies how to perform partial summations or phenomenological adaptations are investigated by several groups [16–18, 21, 22]. A straightforward application of chiral perturbation theory to QCD lattice simulations appears futile (see e.g. [1, 2, 5, 8, 21]).

Recently, systematic analyses of lattice data at N³LO were performed [25–30], where different versions and renormalization schemes for the relativistic chiral Lagrangian were applied. While in [25–27] the $\chi\overline{MS}$ scheme of [16] was used, the EOMS of [31] was used in [29, 30]. Both schemes protect the analytic structure of the one-loop contributions in the baryon self energies as requested by micro causality. In contrast, the IR scheme of [32] was applied in [28]. All three schemes are consistent with the heavy-baryon expansion, and therefore, constitute particular summations of higher order terms. No ad-hoc form factor or cutoff is used in any of those works.

While the works [28–30, 33] consider either the baryon octet or the baryon decuplet masses, a simultaneous description of all baryon states is achieved in [25–27]. There is a further difference as to how the octet and decuplet fields are coupled to the Goldstone bosons. In [25–27] the minimal and traditional form that was shown to be compatible with empirical decay properties of the baryon decuplet decays (see e.g. [16]), was used. The so called ‘consistent’ coupling form suggested in [34, 35] was applied in [29, 30]. The latter form was not used in [25–27] since it does not seem to be compatible with the empirical decay pattern of the decuplet states.

The available lattice data were reproduced at different levels. A first simultaneous de-

description of the BMW, PACS-CS, HSC, LHPC and QCDSF-UKQCD data was achieved in [25–27]. The 6 parameter scenario of [25–27] demonstrated that it was possible to predict for instance the HSC and QCDSF-UKQCD data in terms of the BMW and PACS-CS data. The idea of a simultaneous description of the lattice data was taken up in [29], where however only the baryon octet data of various lattice groups were fitted in terms of the 19 parameters relevant at $N^3\text{LO}$ in the baryon octet sector. As compared to [25–27] the number of fit parameters increased significantly. This is in part, since in the 6 parameter scenario of [25–27] the symmetry conserving counter terms that enter at $N^3\text{LO}$ were not considered. It is difficult to determine them with a subset of lattice data that have sufficiently large lattice volumes so that finite volume corrections can be neglected. Only when considering lattice data with smaller volumes, like the ones provided by QCDSF-UKQCD or NPLQCD, such counter terms can possibly be determined reliably. A first study of finite volume effects at the $N^3\text{LO}$ was performed in [33], however, with only partial success at smaller volumes. In the follow-up work [29] it was emphasized that in a small lattice volume the baryon decuplet degrees of freedom are needed in a description of the baryon octet masses. Still, even the consideration of that effect did not yet lead to a satisfactory description of the QCDSF-UKQCD results on the 24^3 and 16^3 lattice.

Our work is based on the relativistic chiral Lagrangian with baryon octet and decuplet fields where effects at $N^3\text{LO}$ are considered systematically. Here the leading order (LO) corresponds to the chiral limit of the baryon masses and the NLO effects are linear in the quark masses. The details of the approach are published in [16, 18, 25]. A crucial element of our scheme is the use of physical masses in the one-loop contribution to the baryon self energies. Furthermore, the low-energy constants required at $N^3\text{LO}$ are estimated by sum rules that follow from QCD in the limit of a large number of colors (N_c) [8, 25, 36]. The approach was successfully tested against the available lattice data on the nucleon and omega masses of the BMW group [4]. Adjusting eight low-energy constants to the empirical baryon masses we fitted the remaining 6 parameters to the BMW data for the nucleon and omega. In turn we obtained results [25–27] that are in agreement with the predictions of the PACS-CS, HSC, LHPC and QCDSF-UKQCD groups [1–3, 8, 37].

It is the aim of our present study to extend the works [25–27] by considering finite volume effects and possibly arrive at an accurate description of all QCDSF-UKQCD data on the baryon masses. We do not consider discretization effects since in [38, 39] they were estimated

to be of minor importance only. Furthermore, we would like to test the quality of the large- N_c sum rules as derived in [36] for the symmetry conserving counter terms. Altogether there are 17 such counter terms contributing to the baryon octet and decuplet masses at N³LO. Owing to the sum rules of [36] they can be parameterized in terms of 5 parameters only. Clearly such a study can be performed meaningfully only by a simultaneous consideration of the baryon octet and decuplet masses.

The work is organized as follows. We first derive and present the finite volume effects appropriate for the framework [25–27]. Using large- N_s sum rules we arrive at a 12 parameter scenario, which is confronted with the lattice data on the baryon masses. As a consequence we predict a set of low-energy constants and precise values for the baryon sigma terms. In addition detailed predictions for the baryon masses as currently evaluated by the ETM lattice QCD group are made.

BARYON SELF ENERGIES IN A FINITE VOLUME

We consider the chiral extrapolation of the baryon masses to unphysical quark masses. Assuming exact isospin symmetry, the hadron masses are functions of $m_u = m_d \equiv m$ and m_s . The dependence on the light quark masses may be traded against a dependence on the pion and kaon masses. For a given lattice data set we use the lattice pion and kaon masses to determine the quark masses as predicted by χ PT at the next-to-leading order in a finite cubic volume with $V = L^3$. From [40, 41] we recall

$$\begin{aligned}
m_\pi^2 &= \frac{2 B_0 m}{f^2} \left\{ f^2 + \frac{1}{2} \bar{I}_\pi - \frac{1}{6} \bar{I}_\eta + 16 B_0 \left[(2m + m_s)(2L_6 - L_4) + m(2L_8 - L_5) \right] \right\}, \\
m_K^2 &= \frac{B_0(m + m_s)}{f^2} \left\{ f^2 + \frac{1}{3} \bar{I}_\eta \right. \\
&\quad \left. + 16 B_0 \left[(2m + m_s)(2L_6 - L_4) + \frac{1}{2}(m + m_s)(2L_8 - L_5) \right] \right\}, \\
m_\eta^2 &= \frac{2 B_0(m + 2m_s)}{3 f^2} \left\{ f^2 + \bar{I}_K - \frac{2}{3} \bar{I}_\eta \right. \\
&\quad \left. + 16 B_0 \left[(2m + m_s)(2L_6 - L_4) + \frac{1}{3}(m + 2m_s)(2L_8 - L_5) \right] \right\} \\
&\quad + \frac{2 B_0 m}{f^2} \left[\frac{1}{6} \bar{I}_\eta - \frac{1}{2} \bar{I}_\pi + \frac{1}{3} \bar{I}_K \right] + \frac{128 B_0^2 (m - m_s)^2}{9 f^2} (3L_7 + L_8), \tag{1}
\end{aligned}$$

in terms of the renormalized mesonic tadpole integrals \bar{I}_Q with $Q = \pi, K, \eta$. The latter are computed in the \overline{MS} scheme at a renormalization scale μ with

$$\bar{I}_Q = \frac{m_Q^2}{(4\pi)^2} \log\left(\frac{m_Q^2}{\mu^2}\right) + \frac{1}{4\pi^2} \sum_{\vec{n} \in Z^3}^{\vec{n} \neq 0} \frac{m_Q}{|\vec{x}_n|} K_1(m_Q |\vec{x}_n|) \quad \text{with} \quad \vec{x}_n = L \vec{n}, \quad (2)$$

where $K_n(x) = \text{BesselK}[n, x]$ is the modified Bessel function of second kind in the convention used in Mathematica. For a given set of low-energy parameters f, L_i and values for the pion and kaon masses, the quark masses $B_0 m$ and $B_0 m_s$ together with the eta meson mass can be determined by (1) unambiguously.

There are 4 low-energy constants relevant for the meson masses: the flavour SU(3) chiral limit of the pion decay constant f , together with three combinations

$$\begin{aligned} L_4 - 2 L_6 &= 0.09868 \times 10^{-3}, \\ L_5 - 2 L_8 &= -0.39208 \times 10^{-3}, \\ L_8 + 3 L_7 &= -0.30142 \times 10^{-3}, \end{aligned} \quad (3)$$

where we recall the values used in [25, 36] at the renormalization scale $\mu = 0.77$ GeV. Note that $L_4 - 2 L_6$ is expected to vanish in the large- N_c limit. The values are chosen such that for appropriate choices of $B_0 m$ and $B_0 m_s$ the empirical isospin averages for the pion, kaon and eta masses are recovered if $f = 92.4$ MeV is used. According to the latest determination [42] the low-energy constants suffer from substantial uncertainties. For instance the value of the combination $L_5 - 2 L_8$ may be positive or negative. Also a precise value for f is not known. Note however, that for any given choice of $f, L_4 - 2 L_6$ and $L_5 - 2 L_8$ the value of $L_8 + 3 L_7$ is determined by the eta meson mass. In the following we will initially use the value $f = 92.4$ MeV together with (3). The stability of this assumption will be investigated later on.

We turn to the computation of the baryon masses. The physical mass of a baryon M_B of type B is determined by the condition

$$M_B - \Sigma_B(M_B) = \begin{cases} \bar{M}_{[8]} & \text{for } B \in [8] = \{N, \Lambda, \Sigma, \Xi\} \\ \bar{M}_{[10]} & \text{for } B \in [10] = \{\Delta, \Sigma^*, \Xi^*, \Omega\} \end{cases}, \quad (4)$$

with the self energy of the baryon $\Sigma_B(M_B)$ incorporating all tree-level and loop corrections. Note that in the case of the decuplet a projected self energy can be used as described in [16]. The self energy is split into its tree-level and loop contribution

$$\Sigma_B(M_B) = \Sigma_B^{\text{tree-level}}(M_B) + \Sigma_B^{\text{loop}}(M_B), \quad (5)$$

where all tree-level contributions vanish in the chiral limit. Explicit expression for the baryon self energies can be found in the Appendix of [25]. There are three types of contributions considered. The first class enters at NLO and is parameterized by the renormalized low-energy constants $\bar{b}_0, \bar{b}_D, \bar{b}_F, \bar{d}_0$ and \bar{d}_D . The second class are wave function renormalization terms parameterized by $\bar{\zeta}_0, \bar{\zeta}_D, \bar{\zeta}_F, \bar{\xi}_0$ and $\bar{\xi}_D$. Formally they turn relevant at N³LO. Finally there are the terms that are proportional to the square of the quark masses. In the octet sector they are labelled with $\bar{c}_{0,\dots,6}$ and in the decuplet sector they are labelled with $\bar{e}_{0,\dots,4}$. All such parameters run on the ultraviolet renormalization scale μ . It is determined by the request that the baryon masses are independent on μ , if expanded to second order in the quark masses. In the Appendix A the running of all low-energy constants encountered in this work is provided.

While for the NLO parameters we do not impose any constraints from large- N_c sum rules we do so for the parameters relevant at N³LO. A matching of the chiral interaction terms to the large- N_c operator analysis for the baryon masses in [43] leads to the seven sum rules. We recall from [25]

$$\begin{aligned} \bar{c}_0 &= \frac{1}{2} \bar{c}_1, & \bar{c}_2 &= -\frac{3}{2} \bar{c}_1, & \bar{c}_3 &= 0, \\ \bar{e}_0 &= 0, & \bar{e}_1 &= -2 \bar{c}_2, & \bar{e}_2 &= 3 \bar{c}_2, & \bar{e}_3 &= 3 (\bar{c}_4 + \bar{c}_5), \end{aligned} \quad (6)$$

valid at NNLO in the expansion. Assuming the approximate validity of (6) at $\mu = M_{[8]}$, it suffices to determine the five parameters $\bar{c}_4, \bar{c}_5, \bar{c}_6$ and \bar{e}_1, \bar{e}_4 . Analogous relations can be used for the wave-function renormalization terms. As in [25] we apply the following sum rules

$$\bar{\zeta}_D + \bar{\zeta}_F = \frac{1}{3} \bar{\xi}_D, \quad \bar{\zeta}_0 = \bar{\xi}_0 - \frac{1}{3} \bar{\xi}_D. \quad (7)$$

The parameters $\bar{M}_{[8]}$ and $\bar{M}_{[10]}$ are the renormalized and scale-independent bare masses of the baryon octet and decuplet. They do not coincide with the chiral SU(3) limit of the baryon masses. The latter are determined by a set of nonlinear and coupled equations

$$\begin{aligned} M &= \bar{M}_{[8]} - \frac{5 C^2}{768 \pi^2 f^2} \frac{\Delta^3 (2 M + \Delta)^3}{M^2 (M + \Delta)^2} \left\{ M + \Delta \right. \\ &\quad \left. + \frac{2 M (M + \Delta) + \Delta^2}{2 M} \right\} \log \frac{\Delta^2 (2 M + \Delta)^2}{(M + \Delta)^4}, \\ M + \Delta &= \bar{M}_{[10]} - \frac{C^2}{384 \pi^2 f^2} \frac{\Delta^3 (2 M + \Delta)^3}{(M + \Delta)^4} \left\{ M \right. \end{aligned}$$

$$+ \frac{2 M (M + \Delta) + \Delta^2}{2 (M + \Delta)} \Bigg\} \log \frac{M^4}{\Delta^2 (2 M + \Delta)^2}, \quad (8)$$

where we identified the baryon octet and decuplet masses in the one-loop self energy with M and $M + \Delta$ respectively. The parameter C characterizes the octet decuplet transition coupling strength to a Goldstone boson [16]. We will return to its numerical value below.

The loop contributions of the baryon self energies were computed before in the infinite volume limit [16, 25]. Within the $\chi\overline{M}S$ scheme it suffices to compute, besides the tadpole integral, a subtracted scalar bubble-loop integral $\bar{I}_{QR}(M_B)$, which depends on a meson mass m_Q of type $Q \in [8] = \{\pi, K, \eta\}$ and baryon masses $M_{R,B}$ of type $R, B \in [8] = \{N, \Lambda, \Sigma, \Xi\}$ or $R, B \in [10] = \{\Delta, \Sigma^*, \Xi^*, \Omega\}$. It takes the form

$$\begin{aligned} \bar{I}_{QR}(M_B) &= \frac{1}{16\pi^2} \left\{ \left(\frac{1}{2} \frac{m_Q^2 + M_R^2}{m_Q^2 - M_R^2} - \frac{m_Q^2 - M_R^2}{2 M_B^2} \right) \log \left(\frac{m_Q^2}{M_R^2} \right) \right. \\ &\quad + \frac{p_{QR}}{M_B} \left(\log \left(1 - \frac{M_B^2 - 2 p_{QR} M_B}{m_Q^2 + M_R^2} \right) - \log \left(1 - \frac{M_B^2 + 2 p_{QR} M_B}{m_Q^2 + M_R^2} \right) \right) \Bigg\} \\ &\quad + \Delta \bar{I}_{QR}(M_B), \\ p_{QR}^2 &= \frac{M_B^2}{4} - \frac{M_R^2 + m_Q^2}{2} + \frac{(M_R^2 - m_Q^2)^2}{4 M_B^2}, \end{aligned} \quad (9)$$

where the term $\Delta \bar{I}_{QR}(M_B)$ vanishes in the infinite volume limit. Here the computation of the finite volume correction requires special care [23, 44–46]. Depending on the specific values of the meson and baryon masses, power-law contributions in $1/L$ arise. This is contrasted to the exponential behaviour of the Bessel function in the tadpole integral (2). It is necessary to discriminate two cases here. For subthreshold conditions with $M_B < m_Q + M_R$ we find

$$\begin{aligned} \Delta \bar{I}_{QR} &= \frac{1}{8\pi^2} \sum_{\vec{n} \in Z^3}^{\vec{n} \neq 0} \left(\int_0^1 dz K_0(|x_n| \mu(z)) - \frac{2m_Q K_1(|\vec{x}_n| m_Q)}{|x_n| (M_R^2 - m_Q^2)} \right), \\ \mu^2(z) &= z M_R^2 + (1 - z) m_Q^2 - (1 - z) z M_B^2, \quad \vec{x}_n = L \vec{n}, \end{aligned} \quad (10)$$

with finite volume effects exponentially suppressed. Lüscher's power-law terms [44] arise for $M_B > M_R + m_Q$. In this case we find three distinct contributions

$$\begin{aligned} \Delta \bar{I}_{QR} &= -i \frac{p_{QR}}{8\pi M_B} + \frac{1}{8\pi^2 L M_B} Z_{00} \left(1, \frac{L^2}{4\pi^2} p_{QR}^2 \right) \\ &\quad + \frac{1}{2\pi^2} \Re \sum_{\vec{n} \in Z^3}^{\vec{n} \neq 0} \int_0^{+\infty} d\lambda \frac{\lambda}{|x_n|} e^{-\lambda |x_n|/\sqrt{2}} e^{+i\lambda |x_n|/\sqrt{2}} f(\lambda^2). \end{aligned} \quad (11)$$

The first contribution in (11) exactly cancels the imaginary part of (9) that arises for $M_B > M_R + m_Q$. The second term is given by Lüscher's zetafunction

$$Z_{00}(1, k^2) = \sqrt{\pi}^3 \sum_{n \in Z^3}^{|n| \neq 0} \int_0^1 \frac{dt}{\sqrt{t}^3} e^{+t k^2 - 4\pi^2 \vec{n}^2/t} + \sum_{\vec{n} \in Z^3}^{|n| \neq |k|} \frac{e^{-\vec{n}^2 + k^2}}{\vec{n}^2 - k^2} + \sqrt{\pi}^3 \left\{ -2 + \int_0^1 \frac{dt}{\sqrt{t}^3} \left(e^{+t k^2} - 1 \right) \right\}, \quad (12)$$

which we rewrote into a form that is particularly suitable for a numerical evaluation [46]. Finally, the third term specifies further exponentially suppressed contributions, which we expressed in terms of the function

$$f(\lambda^2) = \frac{1}{2} \frac{1}{E_Q E_R (E_Q + E_R)} \frac{M_B^2}{(E_Q + E_R)^2 - M_B^2}, \\ E_Q = \sqrt{m_Q^2 + i \lambda^2}, \quad E_R = \sqrt{M_R^2 + i \lambda^2}. \quad (13)$$

We point out that in a strict chiral expansion of the bubble loop (9) the baryon masses M_B and M_R are expanded around M . This implies that the condition $M_B > M_R + m_Q$ is never met. Therefore Lüscher's finite power-law terms do not arise in any of the computations [29, 30, 33]. This is contrasted by the lattice results that indeed satisfy the condition $M_B > M_R + m_Q$ for various cases in the decuplet sector. It is an important property of our self consistent scheme, in which this dominant and crucial effect is incorporated correctly. Note that even in a case with $M_B < M_R + m_Q$ a chiral expansion of the first term in (10) does not converge.

Before providing explicit expressions for the baryon self energies in a finite box, we address a slight complication. The Passarino-Veltman reduction [47], on which the $\chi\overline{MS}$ scheme rests, requires an additional loop integral, which is needed to express any one-loop diagram in terms of a basis of scalar loop integrals. Since in a finite box Lorentz invariance is lost the reduction formalism of Passarino and Veltman [47] requires an adaptation. This is readily achieved in the case where the three momentum of the baryon is set to zero. The evaluation of the baryon self energy leads to integrals of the type

$$I_{QR}^{(a)}(p_0) = -\frac{i}{V} \sum_{\vec{n} \in Z^3} \int \frac{dk_0}{(2\pi)} \frac{k_0^a}{k^2 - m_Q^2} \frac{1}{k^2 + p_0^2 - 2 p_0 k_0 - M_R^2}, \\ I_Q^{(a)} = \frac{i}{V} \sum_{\vec{n} \in Z^3} \int \frac{dk_0}{(2\pi)} \frac{k_0^a}{k^2 - m_Q^2} \quad \text{with} \quad \vec{k} = \frac{2\pi}{L} \vec{n}, \quad (14)$$

where we are interested in their finite volume effects only

$$\begin{aligned}\Delta I_{QR}^{(a)}(p_0) &= -i \sum_{\vec{n} \in Z^3}^{\vec{n} \neq 0} \int \frac{d^4 k}{(2\pi)^4} \frac{e^{i \vec{x}_n \cdot \vec{k}} k_0^a}{k^2 - m_Q^2} \frac{1}{k^2 + p_0^2 - 2 p_0 k_0 - M_R^2}, \\ \Delta I_Q^{(a)} &= i \sum_{\vec{n} \in Z^3}^{\vec{n} \neq 0} \int \frac{d^4 k}{(2\pi)^4} \frac{e^{i \vec{x}_n \cdot \vec{k}} k_0^a}{k^2 - m_Q^2} \quad \text{with} \quad \vec{x}_n = L \vec{n}.\end{aligned}\quad (15)$$

In contrast to the divergent integrals (14) the integrals (15) are always finite and well behaved. The renormalization of the divergences was considered in great detail in [16]. Note that additional structures proportional to $(k_0^2 - \vec{k}^2)^a$ need not to be considered separately since it is justified to use the replacement $(k_0^2 - \vec{k}^2)^a \rightarrow m_Q^{2a}$ in the integrals (15). This is quite immediate for the tadpole type integral $\Delta I_Q^{(a)}$ but not so obvious for the $\Delta I_{QR}^{(a)}(p_0)$ term. The substitution would be justified rigorously if the integrals of the form

$$-i \sum_{\vec{n} \in Z^3}^{\vec{n} \neq 0} \int \frac{d^4 k}{(2\pi)^4} \frac{e^{i \vec{x}_n \cdot \vec{k}} k_0^a}{k^2 + p_0^2 - 2 p_0 k_0 - M_R^2} = -i \sum_{\vec{n} \in Z^3}^{\vec{n} \neq 0} \int \frac{d^4 k}{(2\pi)^4} \frac{e^{i \vec{x}_n \cdot \vec{k}} (k_0 + p_0)^a}{k^2 - M_R^2}, \quad (16)$$

would vanish. In fact they do not vanish, however, they are suppressed exponentially with $e^{-M_R L}$ and therefore can be neglected safely. If one wishes to keep track of such terms it is useful to observe that they lead to integrals of the form $\Delta I_Q^{(a)}$ with the replacement $m_Q \rightarrow M_R$.

It remains to study the generic integrals $\Delta I_{QR}^{(a)}(p_0)$ and $\Delta I_Q^{(a)}$. We will show that they can be expressed in terms of a specific subset of integrals only. This generalizes the results of Passareno and Veltman for our particular case. Using the identity

$$2 k_0 p_0 = (k^2 - m_Q^2) - (k^2 + p_0^2 - 2 p_0 k_0 - M_R^2) + m_Q^2 + p_0^2 - M_R^2, \quad (17)$$

it follows

$$\begin{aligned}\Delta I_{QR}^{(a)}(p_0) &= \left(\frac{m_Q^2 + p_0^2 - M_R^2}{2 p_0} \right)^n \Delta I_{QR}^{(0)}(p_0) \\ &\quad + \frac{1}{2 p_0} \sum_{k=0}^{a-1} \left(\frac{m_Q^2 + p_0^2 - M_R^2}{2 p_0} \right)^k \Delta I_Q^{(n-k-1)} + \dots,\end{aligned}\quad (18)$$

where we neglect any baryonic tadpole contribution that are exponentially suppressed with $e^{-M_R L}$. The result (18) shows that in fact there it is sufficient to consider $I_{QR}^{(a)}(p_0)$ with $a = 0$ only. It remains to study the tadpole type integrals $I_Q^{(a)}$. We first note that $I_Q^{(a)} = 0$ for a odd. Secondly we observe that in the infinite volume limit all such integrals can be expressed in terms of the renormalized tadpole integral \bar{I}_Q encountered already in (2). Finally we report

that an explicit computation reveals that in our case at hand there are contributions from $\Delta I_Q^{(0)}$ and $\Delta I_Q^{(2)}$ only. Therefore altogether it suffices to consider three master loop integrals, $\bar{I}_{QR}(p_0)$, \bar{I}_Q as studied above in (9, 2) together with the additional independent structure

$$\bar{I}_Q^{(2)} = \frac{1}{4} \frac{m_Q^4}{(4\pi)^2} \log \left(\frac{m_Q^2}{\mu^2} \right) - \frac{1}{4\pi^2} \sum_{\vec{n} \in Z^3}^{\vec{n} \neq 0} \frac{m_Q^2}{|\vec{x}_n|^2} K_2(m_Q |\vec{x}_n|). \quad (19)$$

A comparison of (19) with (2) reveals indeed that in the infinite volume limit we have $m_Q^2 \bar{I}_Q \rightarrow 4 \bar{I}_Q^{(2)}$.

We are now ready to display the baryon self energies in a finite box as implied by the $\chi\overline{MS}$ scheme. They are expressed in terms of the loop integrals \bar{I}_Q , \bar{I}_{QR} and $\bar{I}_Q^{(2)}$. We find

$$\begin{aligned} \Sigma_{B \in [8]}^{\text{loop}} = & \sum_{Q \in [8], R \in [8]} \left(\frac{G_{QR}^{(B)}}{2f} \right)^2 \left\{ \frac{M_R^2 - M_B^2}{2M_B} \bar{I}_Q - \frac{(M_B + M_R)^2}{E_R + M_R} p_{QR}^2 \left(\bar{I}_{QR} + \frac{\bar{I}_Q}{M_R^2 - m_Q^2} \right) \right\} \\ & + \sum_{Q \in [8], R \in [10]} \left(\frac{G_{QR}^{(B)}}{2f} \right)^2 \left\{ \frac{1}{3} \frac{M_B}{M_R^2} \bar{I}_Q^{(2)} - \frac{2}{3} \frac{M_B^2}{M_R^2} (E_R + M_R) p_{QR}^2 \left(\bar{I}_{QR} + \frac{\bar{I}_Q}{M_R^2 - m_Q^2} \right) \right. \\ & \left. + \left(\frac{(M_R - M_B)(M_R + M_B)^3 + m_Q^4}{12 M_B M_R^2} + \frac{4 M_B^2 + 6 M_R M_B - 2 M_R^2}{12 M_B M_R^2} m_Q^2 \right) \bar{I}_Q \right\} \\ & + \frac{1}{(2f)^2} \sum_{Q \in [8]} \left(\left[G_{BQ}^{(X)} - m_Q^2 G_{BQ}^{(S)} \right] \bar{I}_Q - M_B G_{BQ}^{(V)} \bar{I}_Q^{(2)} \right), \end{aligned} \quad (20)$$

with $E_R = \sqrt{M_R^2 + p_{QR}^2}$ and

$$\begin{aligned} \Sigma_{B \in [10]}^{\text{loop}} = & \sum_{Q \in [8], R \in [8]} \left(\frac{G_{QR}^{(B)}}{2f} \right)^2 \left\{ -\frac{1}{3} (E_R + M_R) p_{QR}^2 \left(\bar{I}_{QR} + \frac{\bar{I}_Q}{M_R^2 - m_Q^2} \right) + \frac{1}{6 M_B} \bar{I}_Q^{(2)} \right. \\ & \left. + \left(\frac{(M_R - M_B)(M_R + M_B)^3 + m_Q^4}{24 M_B^3} - \frac{4 M_B^2 + 2 M_R M_B + 2 M_R^2}{24 M_B^3} m_Q^2 \right) \bar{I}_Q \right\} \\ & + \sum_{Q \in [8], R \in [10]} \left(\frac{G_{QR}^{(B)}}{2f} \right)^2 \left\{ -\frac{(M_B + M_R)^2}{9 M_R^2} \frac{2 E_R (E_R - M_R) + 5 M_R^2}{E_R + M_R} p_{QR}^2 \left(\bar{I}_{QR} \right. \right. \\ & \left. \left. + \frac{\bar{I}_Q}{M_R^2 - m_Q^2} \right) + \frac{1}{9 M_R^2 M_B} \left[2 M_B M_R + M_R^2 - M_B^2 \right] \bar{I}_Q^{(2)} \right. \\ & \left. + \left(\frac{M_R^4 + M_B^4 + 12 M_R^2 M_B^2 - 2 M_R M_B (M_B^2 + M_R^2)}{36 M_B^3 M_R^2} (M_R^2 - M_B^2) \right. \right. \\ & \left. \left. + \frac{(M_B + M_R)^2 m_Q^4}{36 M_B^3 M_R^2} + \frac{4 M_B^4 - 4 M_B^3 M_R + 2 M_B^2 M_R^2 - 2 M_R^4}{36 M_B^3 M_R^2} m_Q^2 \right) \bar{I}_Q \right\} \end{aligned}$$

$$+ \frac{1}{(2f)^2} \sum_{Q \in [8]} \left(\left[G_{BQ}^{(\chi)} - m_Q^2 G_{BQ}^{(S)} \right] \bar{I}_Q - M_B G_{BQ}^{(V)} \bar{I}_Q^{(2)} \right), \quad (21)$$

where the sums in (20, 21) extend over the intermediate Goldstone bosons ($Q \in [8] = \{\pi, \eta, K\}$), the baryon octet ($R \in [8] = \{N, \Lambda, \Sigma, \Xi\}$) and decuplet states ($R \in [10] = \{\Delta, \Sigma^*, \Xi^*, \Omega\}$). In the infinite volume limit the self energies coincide with the previous expression as derived first in [16, 25]. Upon a systematic expansion of the baryon masses in the quark masses we generate the results of strict chiral perturbation theory. The running of the low-energy constants as described in detail in the Appendix guarantees the independence of the baryon masses on the ultraviolet renormalization scale at N³LO.

The coupling constants $G_{QR}^{(B)}$ are determined by the parameters F, D, C and H that characterize the strength of the meson-baryon 3-point vertices in the chiral Lagrangian. Explicit expressions are listed in [16]. The parameters F and D follow from a study of semi-leptonic decays of baryon octet states, $B \rightarrow B' + e + \bar{\nu}_e$. This leads to $F \simeq 0.45$ and $D \simeq 0.80$ (see e.g. [48]), the values used in this work. Our value of $C \simeq 1.6$ is determined by the hadronic decays of the decuplet baryons (see e.g. [16]). The parameter H is poorly determined by experimental data so far. Using large- N_c sum rules, the parameters C and H are estimated in terms of the empirical values for F and D [49]. It holds

$$H = 9F - 3D, \quad C = 2D, \quad (22)$$

at subleading order in the $1/N_c$ expansion.

The coupling constants $G_{QR}^{(\chi)}$ probe the renormalized symmetry breaking parameters $\bar{b}_0, \bar{b}_D, \bar{b}_F, \bar{d}_0$ and \bar{d}_D , which entered already the tree-level contribution in (5). They are detailed in Table I of [25]. We are left with 17 symmetry conserving low-energy constants that determine the coupling constants $G_{QR}^{(S)}$ and $G_{QR}^{(V)}$. They do not depend on the renormalization scale and are also listed in Table I of [25]. The large number of unknown chiral parameters at this order is reduced by matching the low-energy and the $1/N_c$ expansions of the product of two axial-vector quark currents [36, 50]. The 17 parameters are correlated by the 12 sum rules

$$\begin{aligned} g_F^{(S)} &= g_0^{(S)} - \frac{1}{2} g_1^{(S)}, & h_1^{(S)} &= 0, & h_2^{(S)} &= 0, & h_3^{(S)} &= \frac{3}{2} g_0^{(S)} - \frac{9}{4} g_1^{(S)} + \frac{1}{2} g_D^{(S)}, \\ h_4^{(S)} &= 3 \left(g_D^{(S)} + \frac{3}{2} g_1^{(S)} \right), & h_5^{(S)} &= g_D^{(S)} + 3 g_1^{(S)}, & h_6^{(S)} &= -3 \left(g_D^{(S)} + \frac{3}{2} g_1^{(S)} \right), \\ g_D^{(V)} &= -\frac{3}{2} g_1^{(V)}, & g_F^{(V)} &= g_0^{(V)} - \frac{1}{2} g_1^{(V)}, & h_1^{(V)} &= 0, & h_2^{(V)} &= \frac{3}{2} g_0^{(V)} - 3 g_1^{(V)}, \end{aligned}$$

$$h_3^{(V)} = \frac{3}{2} g_1^{(V)}, \quad (23)$$

leaving only the five unknown parameters, $g_0^{(S)}, g_1^{(S)}, g_D^{(S)}$ and $g_0^{(V)}, g_1^{(V)}$.

We summarize the number of unknown parameters relevant in the baryon octet and decuplet sector. At N³LO there are altogether 20 parameters if we apply the large- N_c relations (6, 7, 23).

LOW-ENERGY PARAMETERS FROM LATTICE DATA

Our primary goal is the reliable extraction of the low-energy constants from the current lattice data set on the baryon masses. Therefore our analyses rely on the empirical and very precise values for the baryon octet and decuplet masses. Since we do not consider isospin breaking effects nor electromagnetic corrections in our work, we adjust the subset of eight parameters

$$\bar{b}_0, \bar{b}_D, \bar{b}_F, \bar{d}_0, \bar{d}_D, \bar{e}_1, \bar{\zeta}_D, \bar{\xi}_D, \quad (24)$$

to the isospin averaged baryon masses. The particular subset (24) is well suited for that purpose, since for given values of the remaining low-energy constants the parameters are determined by the solution of a linear system.

The use of the empirical baryon masses as suggested in [25–27] constitutes a significant simplification. Rather than a fit with 20 free parameters the adjustment of only 12 parameters to the lattice data is required. Here one should recall that for each parameter set the determination of the baryon masses requires the solution of a set of eight non-linear equations that are coupled to each other. We note that the works [29, 30, 33] do not use the physical masses in the loop contribution of the baryon self energy and therefore can not always describe finite volume effects in a reliable and controlled manner.

In the previous works [25–27] only a subset of the 12 parameters were adjusted to a subset of available lattice data. Data points at small volumes were not considered since the finite volume corrections were not implemented yet. As emphasized before though the subset of lattice data at large volumes can be recovered quite accurately, in such a scheme not all low-energy constants can be determined reliably. Therefore in the scenario of [25–27] all the symmetry preserving parameters that enter at N³LO were put to zero. That left 6 free parameters only that were adjusted successfully to the data of 5 different lattice groups.

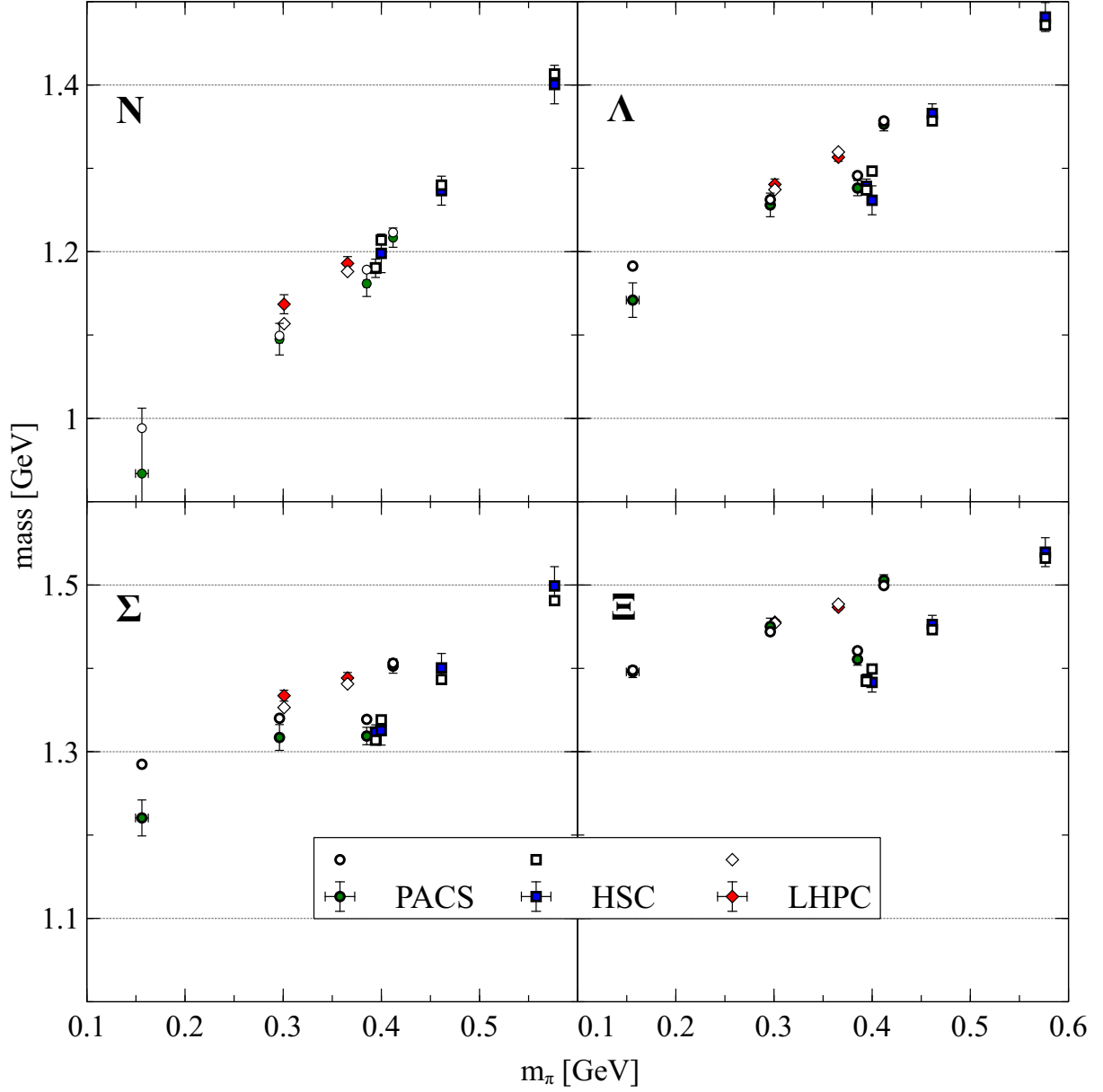


FIG. 1. Baryon octet masses compared with lattice data from PACS-CS, HSC and LHPC. The open symbols give the result of our global fit with $\chi^2/N \simeq 1.73, 0.73, 1.93$ respectively.

Moreover it turned out that one parameter, ξ_0 , could not be determined since its impact on the chi-square function was negligible. So in turn, with in fact only 5 relevant parameters the large volume lattice data were reproduced with a typical $\chi^2/N \sim 1 - 2$. A remarkable success of the chiral extrapolation that illustrates the consistency of the lattice data from 5 different groups.

In the current work we attempt to determine the full set of low-energy parameters and

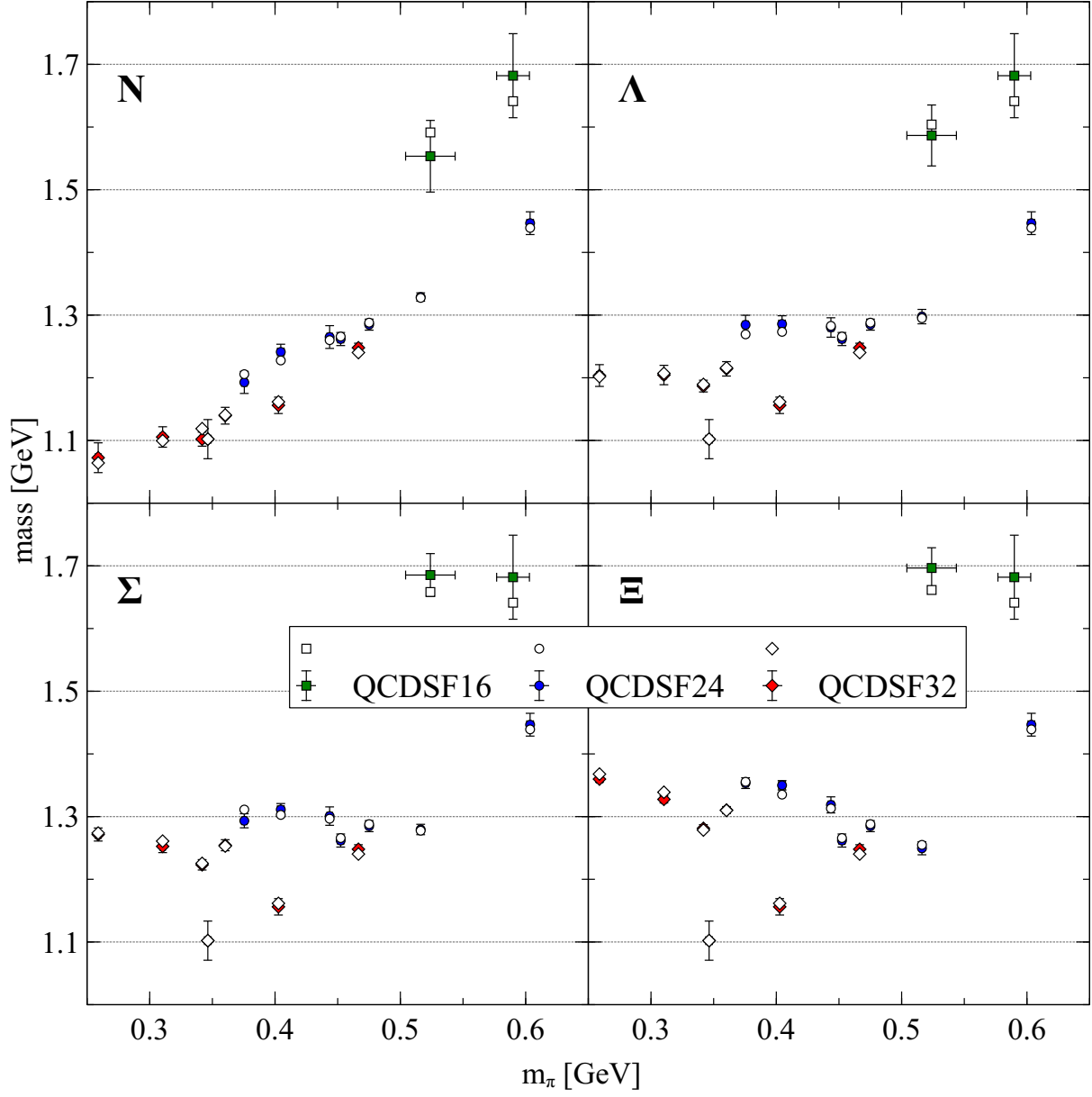


FIG. 2. Baryon octet masses compared with lattice data from QCDSF-UKQCD. The open symbols give the result of our global fit with $\chi^2/N \simeq 0.48, 0.48, 0.56$ for the $16^3, 24^3, 32^3$ lattices respectively.

fit the 12 parameters to the available lattice data set. We form the chi-square

$$\chi^2 = \sum_{i=1}^N \left(\frac{M_i^{\text{Lattice}} - M_i^{\text{EFT}}}{\Delta M_i} \right)^2, \quad (25)$$

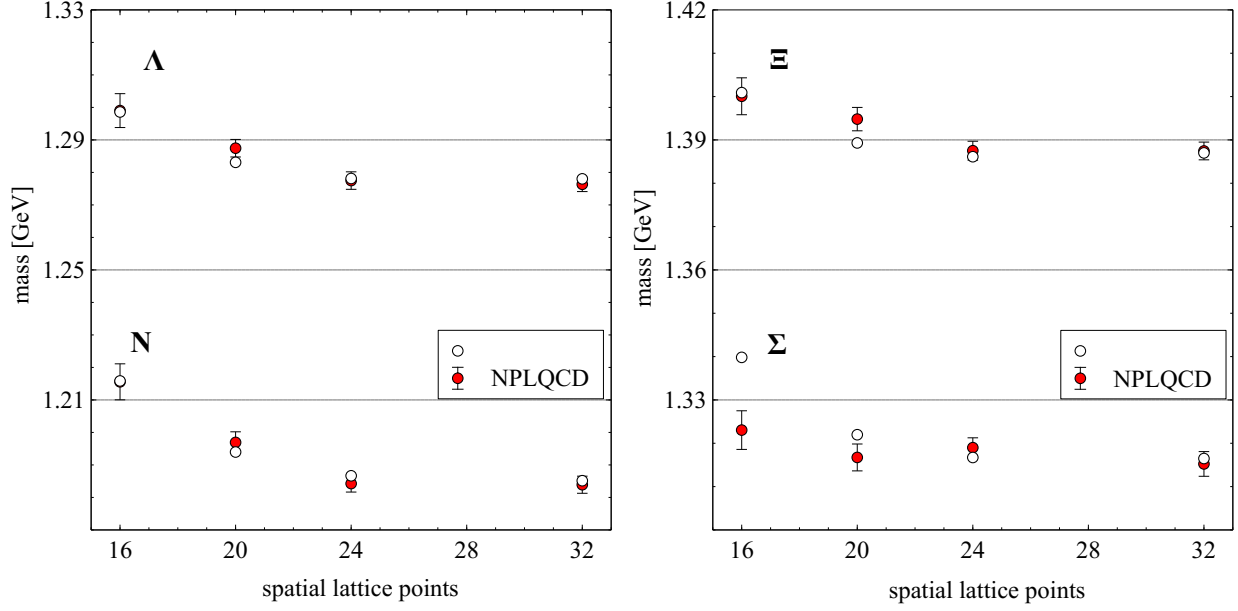


FIG. 3. Baryon octet masses compared with lattice data from NPLQCD. The open symbols give the result of our global fit with $\chi^2/N \simeq 1.75$.

where we take the error $(\Delta M_i)^2$ to be the squared sum of statistical and systematic errors

$$(\Delta M_i)^2 = (\Delta M_i^{\text{statistical}})^2 + (\Delta M_i^{\text{systematic}})^2. \quad (26)$$

We recall that the latter assumption is justified only if the two types of errors are uncorrelated. While the statistical error can be taken from the respective lattice group, the systematic error is poorly known. There are several sources for the latter. Since the available lattice data are evaluated at one lattice spacing only there is an error due to the continuum limit extrapolation. Furthermore, there is an error due to the extraction of the baryon masses from the asymptotic behavior of their correlation function. One would expect the error to be systematically larger for the decuplet as compared to the octet masses. Finally, there must also be a residual uncertainty from the chiral extrapolation at $N^3\text{LO}$.

Additional correlated errors stem from an uncertainty in the determination of the lattice scales of the various groups. Such errors must not be included in the chi-square function via (25). In previous works [21, 23, 29, 30, 33] a different chi-square function was formed

$$\chi_{\text{correlated}}^2 = \sum_{i,j=1}^N (M_i^{\text{Lattice}} - M_i^{\text{EFT}}) \left[C^{(-1)} \right]_{ij} (M_j^{\text{Lattice}} - M_j^{\text{EFT}}), \quad (27)$$

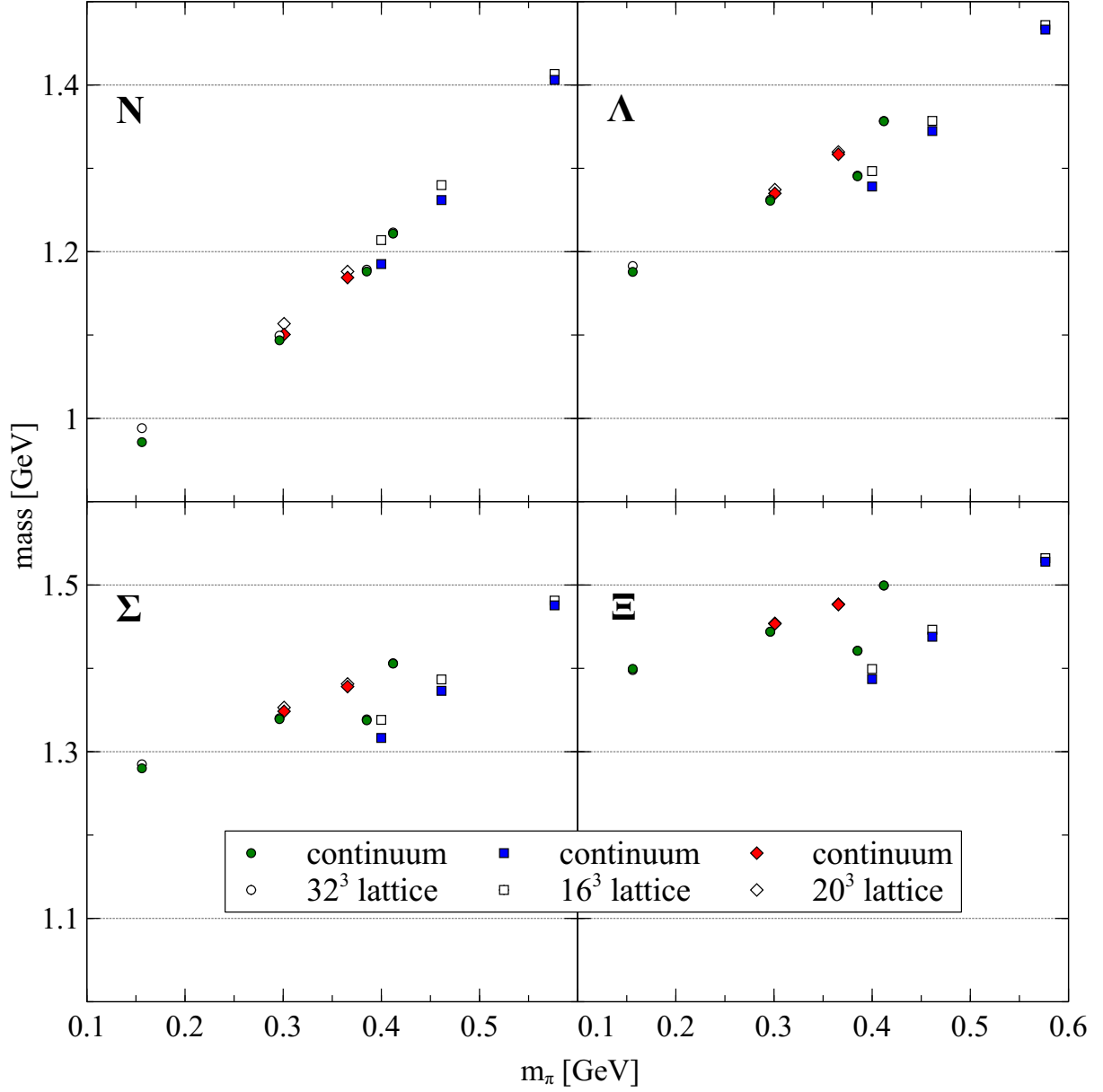


FIG. 4. The size of finite volume effects for the baryon octet masses, where the parameter set 1 is used. The open symbols are recalled from Fig. 1 and show the results including finite volume effects, the corresponding solid points show the masses in the infinite volume limit.

with the correlation matrix

$$C_{ij} = \delta_{ij} \Delta M_i^{\text{statistical}} \Delta M_i^{\text{statistical}} + \Delta M_i^{\text{scale}} \Delta M_j^{\text{scale}}, \quad (28)$$

being computed in terms of the error $\Delta M_j^{\text{scale}}$ that is implied by the scale uncertainty. We would argue that such a treatment is not necessarily always adequate, since it neglects

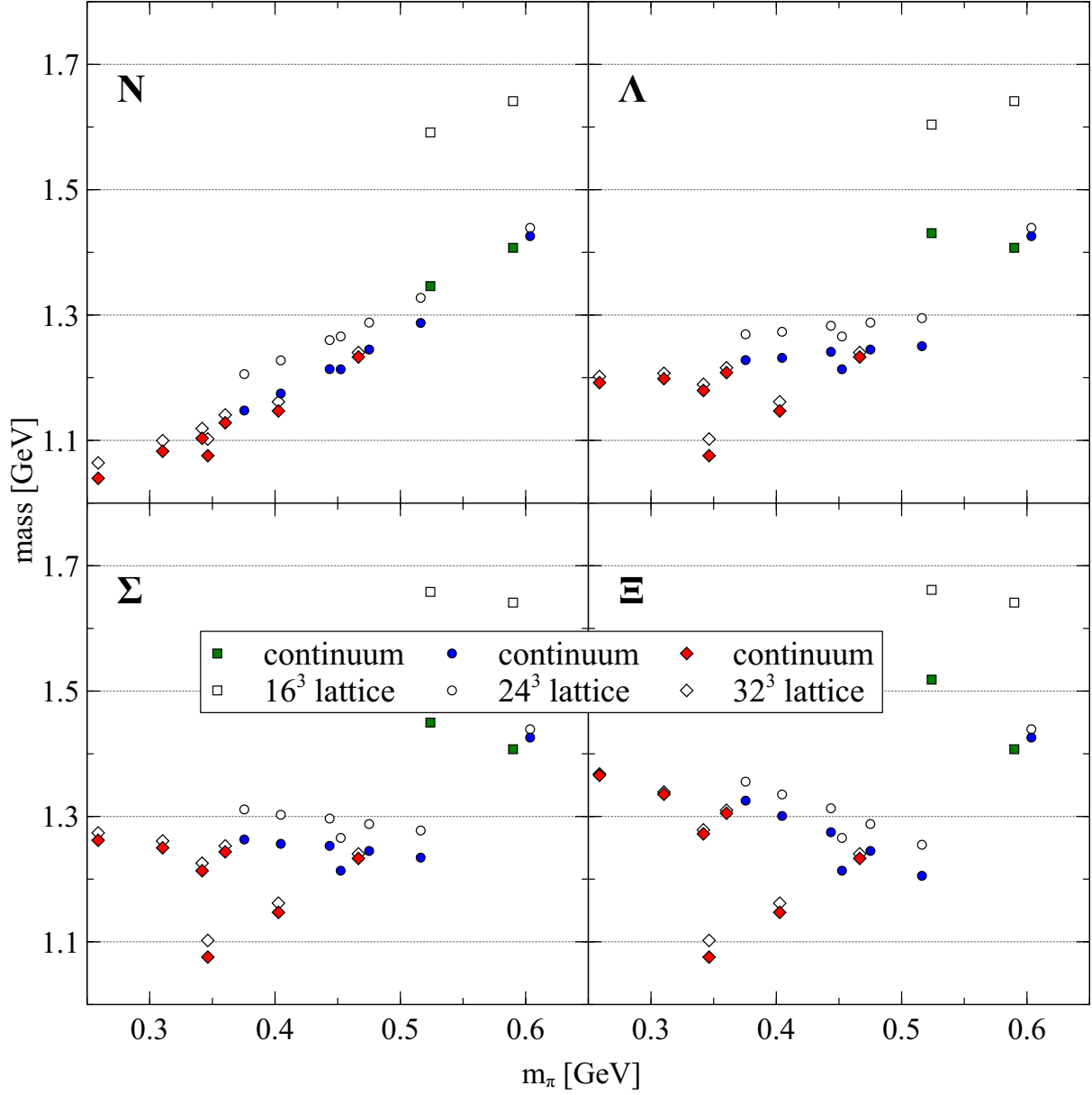


FIG. 5. The size of finite volume effects for the baryon octet masses, where the parameter set 1 is used. The open symbols are recalled from Fig. 2 and show the results including finite volume effects, the corresponding solid points show the masses in the infinite volume limit.

the correlation implied by the quark mass determination via (1). The baryon masses are sensitive to the precise quark masses as obtained from the lattice pion and kaon masses. Clearly, this procedure depends on the lattice scale assumed.

In our scheme we can avoid this issue altogether by including the lattice scales of the various groups as free fit parameters. In turn our chi-square function is defined with (25),

	Fit 1	Fit 2	Fit 3	Fit 4
$\bar{M}_{[8]} \text{ [GeV]}$	0.6370	0.6425	0.6211	0.6171
$\bar{M}_{[10]} \text{ [GeV]}$	1.1023	1.1129	1.1013	1.1080
$\bar{\xi}_0 \text{ [GeV}^{-2}\text{]}$	0.9698	0.9722	0.8284	0.8234
$c_4 \text{ [GeV}^{-3}\text{]}$	-0.1051	-0.1054	-0.1157	-0.0625
$c_5 \text{ [GeV}^{-3}\text{]}$	-0.0822	-0.0809	-0.0590	-0.0748
$c_6 \text{ [GeV}^{-3}\text{]}$	-0.7535	-0.7485	-0.8542	-0.9313
$e_4 \text{ [GeV}^{-3}\text{]}$	-0.3990	-0.4079	-0.3948	-0.4270
$g_0^{(S)} \text{ [GeV}^{-1}\text{]}$	-7.5891	-7.5425	-7.8378	-7.9790
$g_1^{(S)} \text{ [GeV}^{-1}\text{]}$	5.9615	6.0975	6.3602	4.8148
$g_D^{(S)} \text{ [GeV}^{-1}\text{]}$	-3.4955	-3.5833	-3.4694	-3.0003
$g_0^{(V)} \text{ [GeV}^{-2}\text{]}$	5.5127	5.3849	3.8422	4.2322
$g_1^{(V)} \text{ [GeV}^{-2}\text{]}$	-5.2967	-5.3606	-6.0160	-5.3309
χ^2/N	1.255	1.266	1.238	1.263
		1.020		1.019

TABLE I. The parameters are adjusted to reproduce the baryon octet and decuplet masses from the PACS-CS, HSC, LHPC, QCDSF-UKQCD and NPLQCD groups as described in the text. The remaining low-energy parameters are determined by the large- N_c sum rules (6, 7, 22, 23) together with the condition that the isospin averaged masses of the physical baryon octet and decuplet states are reproduced exactly.

where only statistical and uncorrelated systematical errors are required. Here we assume that the unknown systematical errors, to which we will return below, are uncorrelated. The constraint, that we always reproduce the empirical baryon masses, allows us to do so and perform our own scale setting. In the previous work [26] it was demonstrated that for instance the chi-square for the QCDSF-UKQCD data is a very steep function in the lattice

scale. The given uncertainty in the lattice scale leads to a large and significant variation of the chi-square, with a typical range of $2 < \Delta\chi^2/N < 10$. It was argued in [26] that ultimately a controlled chiral extrapolation of the baryon masses, indeed may lead to a very precise determination of the lattice scale.

Finally, before starting a parameter search we have to state our assumption for the systematic errors. In the absence of a solid estimate of the latter, we will let float their size. First, we will perform fits, where only statistical errors are considered. From the quality of such fits we may get a hint about the size of the systematic errors. In a second step we will redo such fits where we assume a non-vanishing systematic but uncorrelated error in order to lower the optimal chi-square down to about $\chi^2/N \simeq 1$. We will assume universal errors for the octet and decuplet masses. A first rough estimate for the expected size follows from the isospin splitting in the baryon masses. Since our scheme and also the lattice groups assume perfect isospin symmetry, such an estimate should constitute a lower boundary for the systematic errors. The isospin splitting of the baryon octet masses is in the range of about 1-4 MeV. A similar range is observed for the decuplet masses. The uncertainty in the low-energy parameters will be deduced from a variation of parameters as they come out of the fits with different sizes of the systematic error.

We take all data points from PACS-CS, HSC, LHPC, QCDSF-UKQCD and NPLQCD into account with a pion mass smaller than about 600 MeV. In the Figs. 1- 7 the lattice data are shown in physical units using already the optimal lattice scales as they come out of our fit. We chose a representation linear in the pion mass as to highlight the approximate linearity of the baryon masses in that parameter [1, 51–53]. The scattering of the different lattice points reflects different choices for the kaon masses. Our chi-square functions exclude the data points of the BMW collaboration since they are not made available publicly. A comparison with their nucleon and omega mass as displayed in a figure of [4] for their smallest lattice spacing will be provided below nevertheless. Finally we exclude all data points from LHPC on the decuplet states, with the exception of the omega baryon. We found no way to reproduce the Δ , Σ^* and Ξ^* masses in any of our fits and therefore consider them as outliers. The consequence of our best fit will be confronted with those data points also.

Stable results for the low-energy constants require a simultaneous fit of all data points included in our chi-square function. Leaving out for instance the octet data from LHPC leaves a rather flat valley in the chi-square function along which the low-energy parameters

		Fit 1	Fit 2	Fit 3	Fit 4	Lattice Result
a_{QCDSF}	[fm]	0.07389	0.07405	0.07368	0.07412	0.0765(15) [7]
a_{HSC}	[fm]	0.03410	0.03417	0.03405	0.03423	0.0351(2) [3]
a_{LHPC}	[fm]	0.12080	0.12125	0.12072	0.12122	0.1241(25) [54]
a_{PACS}	[fm]	0.09055	0.09061	0.09045	0.09053	0.0907(14) [2]
f	[MeV]	92.4	92.4	89.5	88.1	
$10^3 (L_4 - 2 L_6)$		0.099	0.099	0.110	0.092	
$10^3 (L_5 - 2 L_8)$		-0.392	-0.392	-0.393	-0.357	
F		0.450	0.450	0.436	0.427	
D		0.800	0.800	0.802	0.785	

TABLE II. Our determination of the lattice scale for QCDSF-UKQCD, HSC, LHPC and PACS. The values of the additional five low-energy parameters that were activated in Fit 3 and Fit 4 are shown.

may change significantly. A determination of the symmetry conserving parameters relevant at N³LO is most sensitive to the QCDSF-UKQCD data on their 16³, 24³ and 32³ lattices and the NPLQCD data for the baryon octet masses on their 16³, 20³, 24³ and 32³ lattices. Since the PACS-CS and HSC data are for quite distinct values of the pion and kaon masses, as compared to QCDSF-UKQCD and NPLQCD, it is crucial to keep their data in the chi-square function also.

In the Figs. 1-9 the results of our best fit are shown and confronted with the data from the various lattice groups. An excellent reproduction is achieved with 12 free parameters only. The total chi-square per number of data point is $\chi^2/N \simeq 1.255$. The corresponding low-energy parameters correspond to Fit 1 in Tab. I. We do not provide any statistical error estimate since they are negligible. This is because we describe more than 220 data points with 12 parameters only. The stability of our solution is studied by assuming an additional systematic error for the octet and decuplet masses of 3 and 6 MeV respectively.

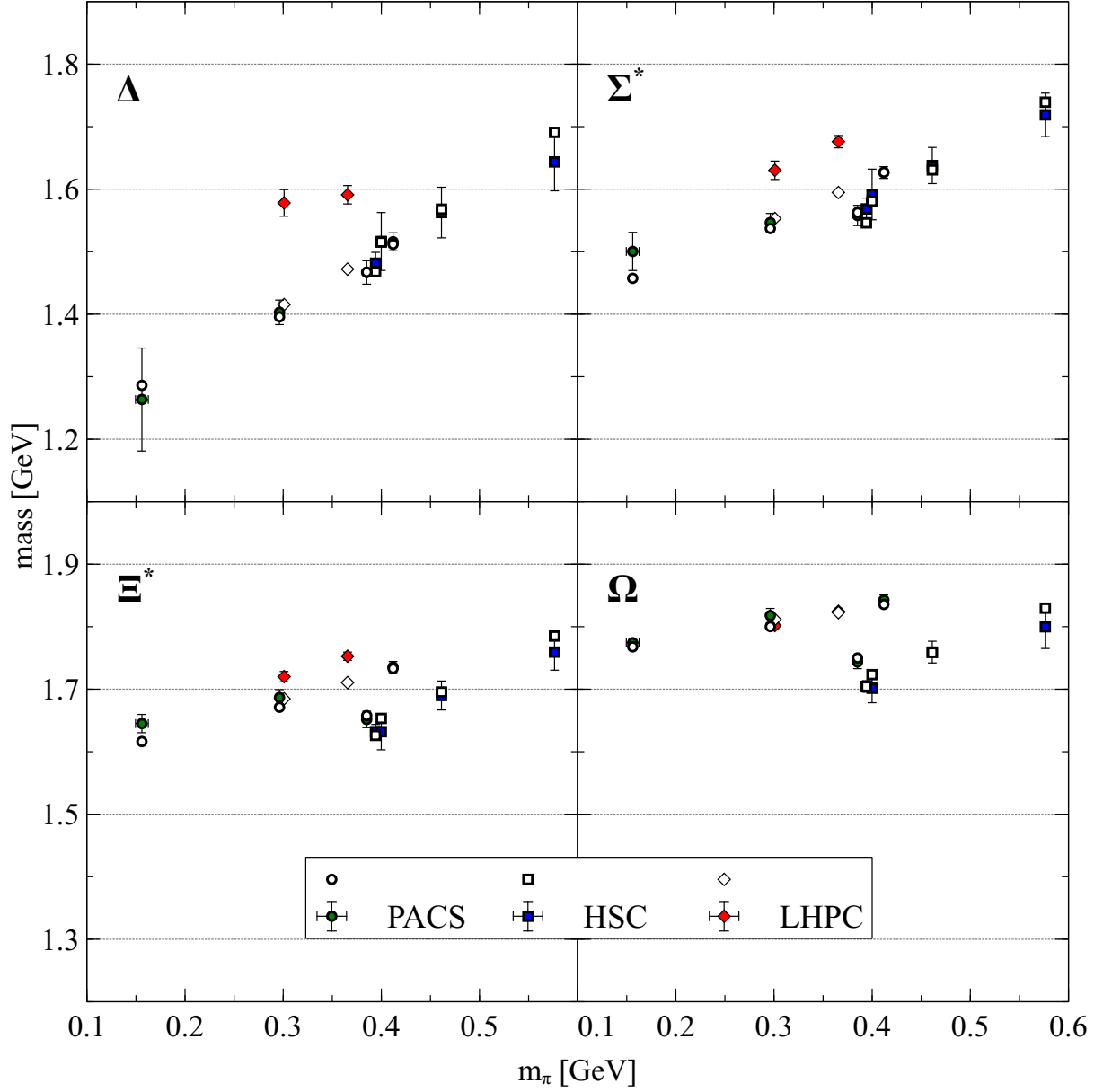


FIG. 6. Baryon decuplet masses compared with lattice data from PACS-CS, HSC and LHPC. The open symbols give the result of our global fit with $\chi^2/N \simeq 0.80, 0.44, 35.7$ respectively. The Δ, Σ^* and Ξ^* masses of the LHP collaboration were not included in our global fits. The chi-square given in Tab. I does not consider the contributions of those outliers.

A new parameter search was performed, which results are shown under Fit 2 in Tab. I. While the $\chi^2/N \simeq 1.020$ is lowered significantly all low-energy parameters have moderate changes only. Taking the Fit 2 parameters we calculate the chi square value in absence of the systematic error. In this case we obtain $\chi^2/N \simeq 1.266$, a value slightly larger than the

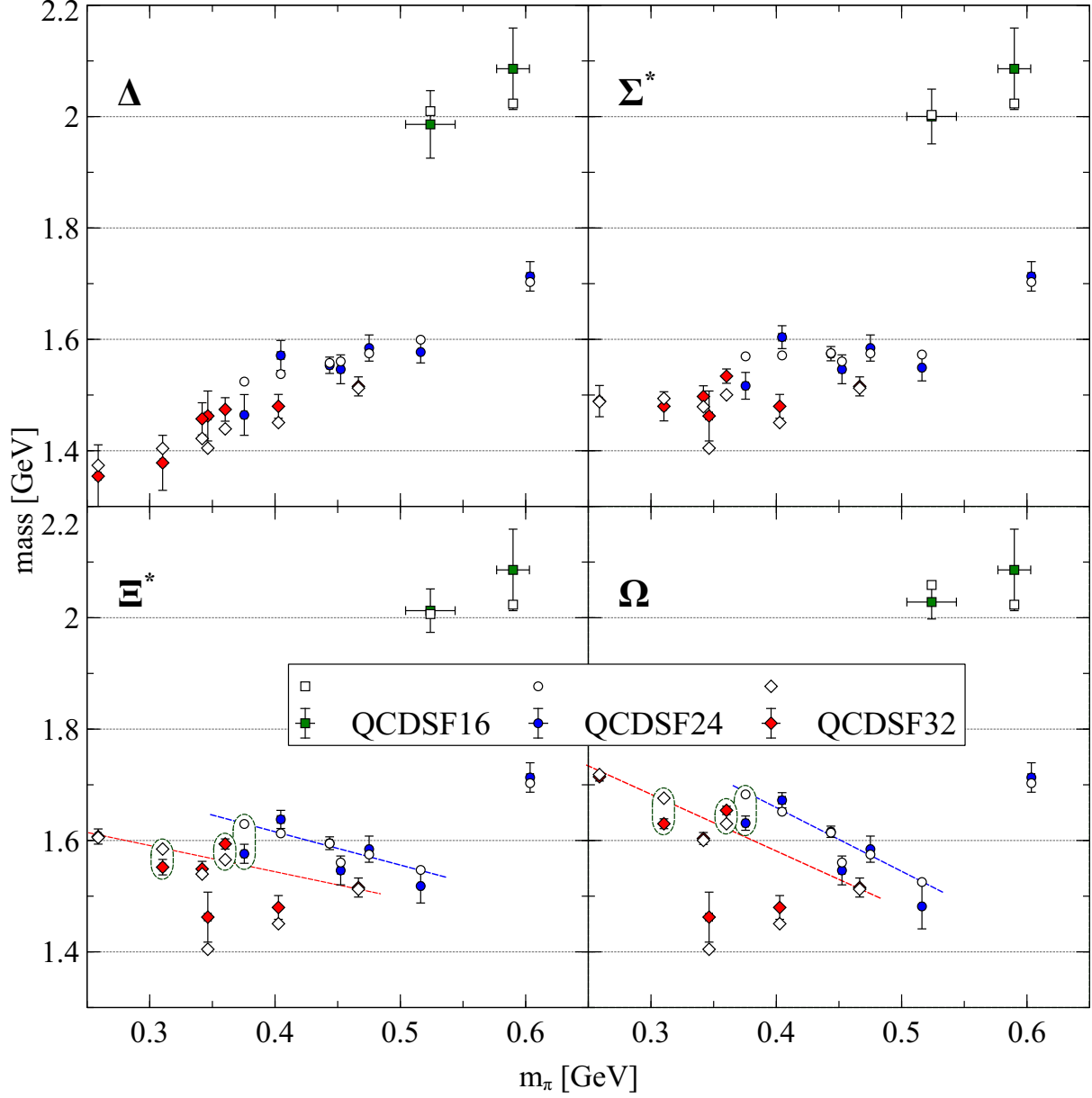


FIG. 7. Baryon decuplet masses compared with lattice data from QCDSF-UKQCD. The open symbols give the result of our fit with $\chi^2/N \simeq 0.51, 1.75, 2.87$ for the $16^3, 24^3, 32^3$ lattices respectively. Along the straight lines the averaged quark mass $2m + m_s$ is approximatively constant. The quark mass ratio $(m_s - m)/(2m + m_s)$ takes the values shown in (30) and (31).

one of Fit 1. With scenario 3 and 4 in Tab. I and Tab. II we illustrate the influence of including 5 extra parameters F, D and $f, L_4 - 2L_6, L_5 - 2L_8$ in the parameter search. While Fit 3 corresponds to the assumption of vanishing systematic errors, the Fit 4 parameters are with respect to the same systematic errors as assumed for Fit 2. Again the low-energy

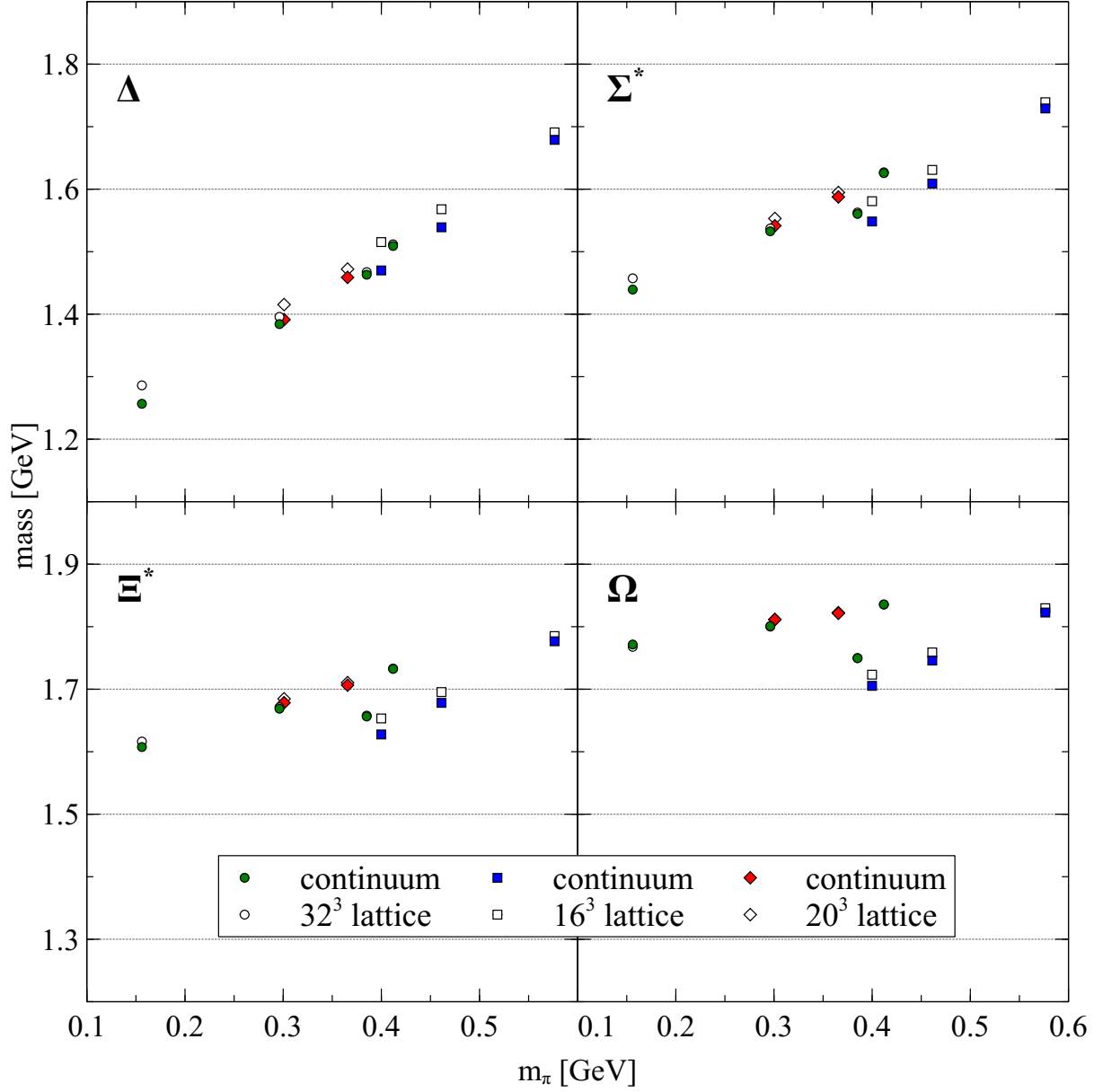


FIG. 8. The size of finite volume effects for the baryon decuplet masses, where the parameter set 1 is used. The open symbols are recalled from Fig. 6 and show the results including finite volume effects, the corresponding solid points show the masses in the infinite volume limit.

parameters shown in Tab.II suffer from moderate variations only. The chi-square for Fit 4 that includes the additional systematic error is $\chi^2/N \simeq 1.019$. The values of the additional five parameters are collected in Tab. II. We observe that the consideration of the extra five parameters does not lower our chi-square value significantly. Our results show that our a priori choices were very reasonable. It is pointed out that the values of the low-energy

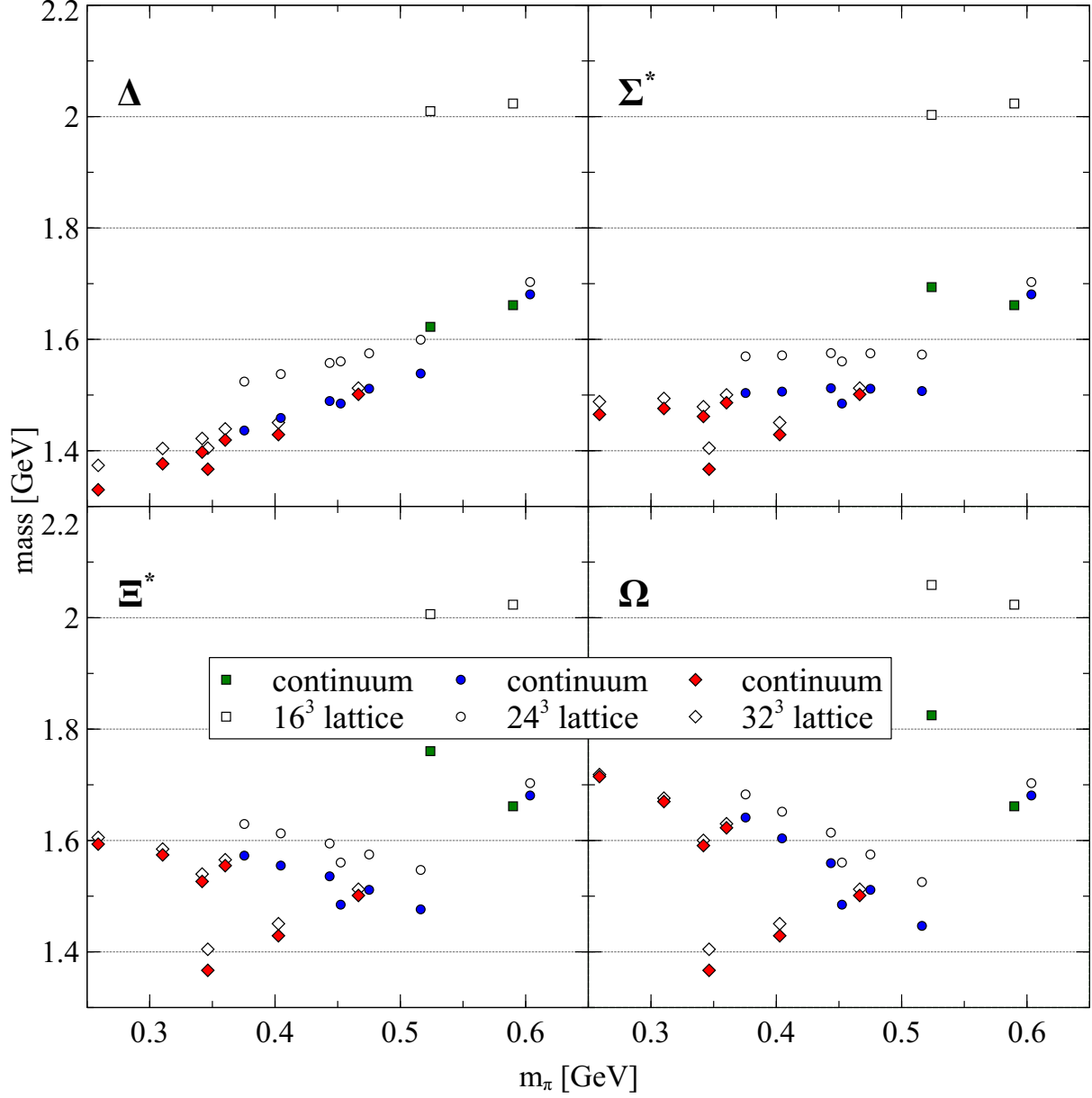


FIG. 9. The size of finite volume effects for the baryon decuplet masses, where the parameter set 1 is used. The open symbols are recalled from Fig. 7 and show the results including finite volume effects, the corresponding solid points show the masses in the infinite volume limit.

constants $f, L_4 - 2L_6, L_5 - 2L_8, F, D$ have a crucial impact on the description of the baryon masses from lattice QCD simulations. For instance if we insisted on a positive value for $L_5 - 2L_8$ we did not find fits of comparable quality. The relevance of physical choices for the F and D parameters was emphasized previously in [8, 26].

The chiral limit values of the baryon octet and decuplet states, M and $M + \Delta$, follow

from the solution of the set of non-linear equations (4). Using the parameters of Tab. I and Tab. II we find the ranges

$$M = (802 \pm 4) \text{ MeV}, \quad M + \Delta = (1103 \pm 6) \text{ MeV}. \quad (29)$$

Our result is compatible with the previous estimates in [26]. Using parameter set 1 of that work we find the values $M \simeq 826 \text{ MeV}$ and $M + \Delta \simeq 947 \text{ MeV}$. The somewhat larger values $M \simeq 903 \text{ MeV}$ and $M + \Delta \simeq 1157 \text{ MeV}$ follow with parameter set 2 of that work.

We remind the reader that our chi-square definition does consider statistical errors as given by the lattice groups only. The uncertainty from the scale setting is considered by keeping the various lattice scales as free parameters. In Tab. II we show the lattice scales as they come out of our four different fits. Note that the lattice scales of the NPLQCD and HSC groups coincide. It is reassuring that we obtain values that are compatible with the scale determination of the lattice groups within their estimated uncertainties. We find remarkable that the variance of the lattice scales found for our 4 different fits is at the five per mil level.

In Figs. 1-3 and Figs. 6-7 a detailed comparison of our Fit 1 results with the lattice data is offered. We affirm that any of the other scenarios would lead to almost indistinguishable figures. In Fig. 1 we confront our results for the baryon octet masses with those of PACS-CS, HSC and LHPC. From our global fit we obtain $\chi^2/N \simeq 1.73, 0.73, 1.93$ respectively, where the chi-square is evaluated according to (25). Only statistical errors are considered. The uncertainties in the lattice scales were taken into account by including the latter into the parameter search. If we instead compute the chi-square with respect to (27) as advocated in [21, 23, 29, 30, 33] we obtain significantly smaller values $\chi^2/N \simeq 1.34, 0.57, 1.69$. From this we conclude that the use of the correlation matrix in the form of (27) is not always adequate.

In Fig. 2 we collected the data from the QCDSF-UKQCD collaboration for the baryon octet masses at three different lattice volumes. Our global description implies chi-square values $\chi^2/N \simeq 0.48, 0.48, 0.56$ with respect to (25) and $\chi^2/N \simeq 0.27, 0.31, 0.27$ with respect to (27). It is noteworthy that the lattice data are well described for all three lattice volumes. This was not possible in the previous works [29, 33], which considered exclusively the four octet masses in terms of fits with their 19 free parameters.

A further important constraint for the low-energy parameters arises from the accurate

data of the NPLQCD group, which we scrutinize in Fig. 3. Our global fit describes the latter with a $\chi^2/N \simeq 1.75$ and $\chi^2/N \simeq 1.46$ according to (25) and (27) respectively. The chi square is largely dominated by an outlier, the sigma baryon mass for the 16^3 lattice.

We conclude our discussion of the baryon octet states with Fig. 4 and Fig. 5 where the importance of the finite volume effects is illustrated. The two figures correspond to the previous Fig. 1 and Fig. 2, only that a comparison of our finite volume results (open symbols) with their infinite volume limits (solid symbols) rather than the lattice data is shown. The figures clearly show the significance of the finite volume corrections, in particular for the data from the QCDSF-UKQCD group on their 24^3 and 16^3 lattice. Note that the size of the finite volume effects does not always decrease with increasing pion mass. This is because the lattice configurations are such that the associated kaon and eta masses are sometimes getting smaller as the pion mass increases. This is the case for the QCDSF-UKQCD data.

We turn to the decuplet masses. In Fig. 6 they are compared with the results of PACS-CS, HSC and LHPC. The two types of chi-squares are $\chi^2/N \simeq 0.80, 0.44, 35.7$ and $\chi^2/N \simeq 0.34, 0.22, 16.1$. While we achieve an excellent description of the PACS-CS and HSC data we fail to recover the Δ , Σ^* and Ξ^* masses of the LHP collaboration. As mentioned before the latter are considered as outliers and consequently were excluded in our definition of the global chi-square functions. From Fig. 6 one may speculate that there is some tension in the data of LHPC as compared to PACS-CS and HSC, at least for the Δ where the slightly different strange quark masses used are expected not to be relevant.

In Fig. 7 we confront our results with the QCDSF-UKQCD simulations for the decuplet masses. We refrain from using a speed plot representation suggested in [7] and also used in previous works [27, 30]. As already shown in [53] not taking the particular ratios required by the fan plots reveals interesting and additional information on the baryon decuplet states. Our description of the lattice is characterized by the following chi-square values $\chi^2/N \simeq 0.51, 1.75, 2.87$ for the 16^3 , 24^3 and 32^3 lattices. Again computing the chi-square using the correlation matrix (28) leads to significantly smaller values $\chi^2/N \simeq 0.26, 0.87, 1.41$. Our reproduction of the QCDSF-UKQCD is characterized by two outliers for the 32^3 lattice and one outlier for the 24^3 lattice. While our description for the more complicated Δ and Σ^* masses is excellent, this is not the case for the description of the Ξ^* and Ω^* masses, for which we encircled the outliers. We find this puzzling since in particular for the Ω there is no available decay channel which may complicate the computation of finite volume effects.

For the 32^3 lattice the chi-square is largely dominated by the 2nd point for the Ξ^* and Ω mass. Such points have a large distance to the dashed lines shown in Fig. 7. The latter lines connect smoothly four distinct open symbols that give the prediction of our extrapolation. Similarly, the 1st point of the 24^3 lattice deviates strongly from the dashed lines drawn for the Ξ^* and Ω masses. In this case the line connects five open symbols. Note that analogous straight lines may be drawn for the Δ and Σ^* in Fig. 7 and also for the baryon octet states in Fig. 2.

An explanation for such a linearity is readily found. The corresponding lattice points are taken at constant averaged quark masses, where the values for $2m + m_s$ are changing by less than 3 per cent on the 32^3 and less than 1 per cent for the 24^3 lattices. On the other hand the quark mass ratio takes the values

$$\frac{m_s - m}{2m + m_s} = \left\{ +0.67, +0.53, +0.38, 0.00 \right\}, \quad (30)$$

along the four particular points on the 32^3 lattice and

$$\frac{m_s - m}{2m + m_s} = \left\{ +0.36, +0.26, +0.16, 0.00, -0.17 \right\}, \quad (31)$$

along the five particular points on the 24^3 lattice. It is an amusing observation that the step size in the symmetry breaking quark mass ratio coincides with the corresponding step size in the pion mass. To this extent the linear behaviour seen in the Fig. 7 is a direct consequence of the well known equal spacing rule for the decuplet masses. An expansion of the decuplet masses in the parameter $m_s - m$ at fixed value of $2m + m_s$ provides an accurate description of the masses already with only the linear term kept. Given our framework there is no way to generate the significant departure of the lattice data for the Ξ^* and Ω masses from the straight dashed lines as shown in Fig. 7. We conclude that the linearity of the decuplet fan plots [7] is in part a subtle consequence of taking particular ratios.

We conclude our discussion of the baryon decuplet states with Fig. 8 and Fig. 9 where the relevance of the finite volume effects is illustrated. The two figures correspond to the previous Fig. 6 and Fig. 7, only that a comparison of our finite volume results (open symbols) with their infinite volume limits (solid symbols) rather than the lattice data is shown. The figures clearly show the importance of the finite volume corrections, in particular for the data from the QCDSF-UKQCD group on their 24^3 and 16^3 lattice. For the 32^3 lattice the corrections are found to be most sizeable for the Δ and Σ^* masses.

		Fit 625	Fit 525	Fit 425A	Fit 425B	Fit 425C
$\bar{M}_{[8]}$	[GeV]	0.63413	0.59844	0.59515	0.59945	0.62992
$\bar{M}_{[10]}$	[GeV]	1.09281	1.09614	1.06418	0.99809	1.03836
$\bar{\xi}_0$	[GeV ⁻²]	1.01089	0.79578	0.75710	0.90093	0.96789
c_4	[GeV ⁻³]	-0.21601	-0.39418	-0.33941	-0.15380	-0.10026
c_5	[GeV ⁻³]	0.02621	0.27852	0.26157	0.15654	-0.04887
c_6	[GeV ⁻³]	-0.68692	-0.37708	-0.38501	-0.55271	-0.70022
e_4	[GeV ⁻³]	-0.38886	-0.35039	-0.30906	-0.22345	-0.31497
$g_0^{(S)}$	[GeV ⁻¹]	-9.23670	-9.47963	-9.33530	-8.72593	-8.21464
$g_1^{(S)}$	[GeV ⁻¹]	6.59741	7.39081	6.89777	7.62471	5.71282
$g_D^{(S)}$	[GeV ⁻¹]	-2.22149	-1.40226	-1.46690	-4.90674	-3.17883
$g_0^{(V)}$	[GeV ⁻²]	6.59077	3.59025	4.43491	7.99845	5.74075
$g_1^{(V)}$	[GeV ⁻²]	-4.53460	-5.67925	-4.58849	-2.90244	-4.83729
a_{QCDSF}	[fm]	0.07401	0.07425	0.07412	0.07423	0.07396
a_{HSC}	[fm]	0.03412	0.03429	0.03430	0.03448	0.03419
a_{LHPC}	[fm]	0.12077	0.12129	0.12176	0.12198	0.12140
a_{PACS}	[fm]	0.09057	0.09094	0.09111	0.09136	0.09091
χ^2/N		0.8857	0.9259	1.1319	1.1326	1.1764
$\chi^2/N @ L = \infty$		6.6783	6.3526	3.4259	3.6110	3.4716

TABLE III. The parameters are adjusted as for Fit 1 of Tab. III. In the chi square function the errors for the encircled 6 points in Fig. 7 are enlarged by an ad-hoc factor of 5 as explained in the text. In addition only subsets of the global lattice data sets are considered. While the first and second column consider lattice data only with $m_\pi < 625$ MeV and $m_\pi < 525$ MeV, the last three columns correspond to the same pion mass cutoff of 425 MeV.

As a further consistency check we performed additional fits where the relevance of the possible outliers in the QCDSF-UKQCD data set as discussed above is reduced. For the encircled 6 points in Fig. 7 we enlarged the error by an ad-hoc factor of 5. Based on such a modified chi square function we performed a series of fits where the size of the global data set is gradually reduced by imposing a cutoff in the maximum pion mass. In order to gauge

such new fits we first evaluate the updated chi square values with respect to our established solution Fit 1 of Tab. 1. We obtain the following values

$$\begin{aligned}
\chi^2/N \Big|_{m_\pi < 625 \text{ MeV}} &= 0.9085 && \text{with } N = 218 \text{ data points ,} \\
\chi^2/N \Big|_{m_\pi < 525 \text{ MeV}} &= 0.9697 && \text{with } N = 194 \text{ data points ,} \\
\chi^2/N \Big|_{m_\pi < 475 \text{ MeV}} &= 1.0508 && \text{with } N = 170 \text{ data points ,} \\
\chi^2/N \Big|_{m_\pi < 425 \text{ MeV}} &= 1.2309 && \text{with } N = 138 \text{ data points ,} \\
\chi^2/N \Big|_{m_\pi < 375 \text{ MeV}} &= 1.2098 && \text{with } N = 66 \text{ data points .} \tag{32}
\end{aligned}$$

As a consequence of the reduced impact of the six outliers the chi square value for the first case with $m_\pi < 625$ MeV is smaller than the corresponding value of Tab. 1 of about 1.26. As can be seen from the various figures discussed above our lattice data description is quite uniform in quality. This is reflected in an only moderate increase of the chi square values as one lowers the pion mass cutoff from 625 MeV down to 375 MeV. Note that this reduces the size of the global data set by about a factor 3. The large step from the 425 MeV case to the 375 MeV case is due to the throw out of the HSC and NPLQCD data sets. Since all chi square values are quite close to one the significance of refits of the parameter set 1 using the updated chi square functions is unclear. In particular, we note that if we supplement the updated chi square functions by the ad-hoc systematical errors of 3 and 6 MeV for all octet and decuplet baryon masses, as used before in Fit 2, the chi square values of (32) would be 1.02 for the $m_\pi < 425$ MeV and 1.04 for the $m_\pi < 375$ MeV case. Nevertheless we show 5 representative refits where the maximum pion mass allowed was fixed to either 625 MeV, 525 MeV or 425 MeV. The results thereof are collected in Tab. III. The last row of the table illustrates the crucial importance of finite volume effects. Switching them off leads to a huge increase of the chi square value.

We observe that our refits lead to only rather moderate improvements in the chi square values. This is seen by a comparison of (32) with the second last row of Tab. III. On the other hand the spread in the parameter variations is larger as seen in Tab. I and II. This is not surprising since reducing the size of the lattice data set may not always lead to a full determination of all low-energy constants. While we expect the chiral extrapolation to work more accurately at smaller quark masses, it is not clear whether a reduced data set with smaller pion masses is sufficient to identify a unique set of parameters. Indeed, our solutions

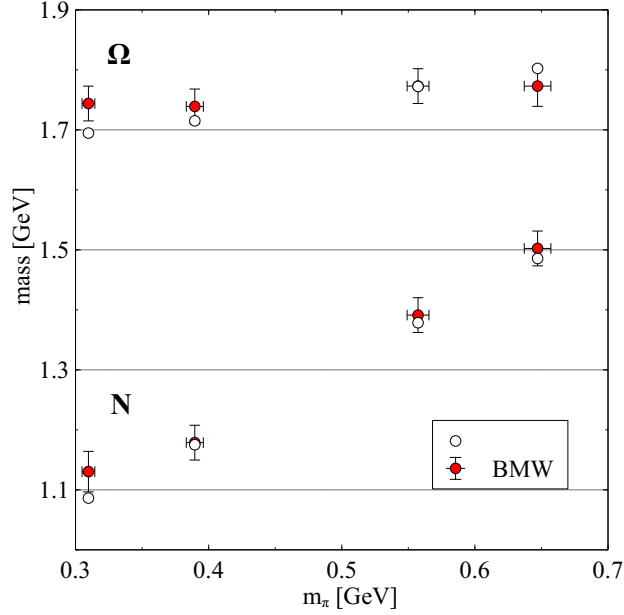


FIG. 10. Masses of the nucleon and omega compared with lattice data from BMW. The open symbols give the prediction of our fit with $\chi^2/N \simeq 0.82$.

425A and 425B have very similar chi square values but significantly different low-energy parameters. This is typical for the considered system. Only with the data set as considered in Fit 1-4 of Tab. I we find reasonably well defined and essentially unique solutions. However, even in this case the chi square function is quite shallow around the established solution and further lattice data may move the solution somewhat. It is interesting to evaluate the chi square of all solutions given in Tab. III with respect to the 'full' data set. While for the 1st column the given chi square value follows, for the last 4 columns we obtain the values 0.90, 0.95, 1.01 and 0.94 respectively. From those values we may conclude that solution 425A is superior over the solutions 425B and 425C.

As a final consistency check of our lattice data description we provide Fig. 10, where our results are compared with the unfitted BMW data as taken from a figure in [4] for their smallest lattice spacing. We use Fit 1 here for which its chi square is estimated with $\chi^2/N \simeq 0.82$. A similar chi square is obtained for Fit 2-4. This gives us further confidence on the reliability of our chiral extrapolation. Unfortunately, corresponding results for the remaining members of the octet and decuplet states are not available publicly. It is interesting to note that the solutions of Tab. III are discriminated by the BMW data. While solution 525A has a chi square of 1.09 solution 425B leads to a significantly worse

	Fit 475A	Fit 475B	Fit 375A	Fit 375B	Fit A
$\bar{M}_{[8]} \text{ [GeV]}$	0.6300	0.9425	0.6356	0.9495	0.6370
$\bar{M}_{[10]} \text{ [GeV]}$	1.1027	1.1894	1.1066	1.2617	1.1023
$\bar{b}_0 \text{ [GeV}^{-1}\text{]}$	-1.3460	-0.2979	-1.3808	-0.2472	-1.4118
$\bar{b}_D \text{ [GeV}^{-1}\text{]}$	0.4957	0.0673	0.4844	0.0446	0.5022
$\bar{b}_F \text{ [GeV}^{-1}\text{]}$	-0.5859	-0.1576	-0.5721	-0.1437	-0.5917
$\bar{d}_0 \text{ [GeV}^{-1}\text{]}$	-0.2956	-0.2482	-0.2789	-0.1503	-0.3303
$\bar{d}_D \text{ [GeV}^{-1}\text{]}$	-0.4569	-0.5441	-0.4496	-0.4582	-0.5196
F	0.4117	0.1062	0.4138	0.1217	0.4500
D	0.7863	-0.1814	0.8096	-0.0386	0.8000
χ^2/N	4.24	3.19	4.25	1.25	61.0
					40.2

TABLE IV. The parameters at N²LO are adjusted to the lattice data as in Tab. III. The large- N_c sum rules $C = 2D$ and $H = 9F - 3D$ together with $f = 92.4$ MeV and $\mu = M_{[8]}$ are used. The fits are performed at fixed lattice scales with $a_{\text{LHPC}} = 0.124$ fm, $a_{\text{HSC}} = 0.035$ fm, $a_{\text{PACS}} = 0.091$ fm and $a_{\text{QCDSF}} = 0.075$ fm.

description with a chi square value of 1.32. An even better description with a chi square value of 0.94 is generated by solution 425C. The first two solutions have chi square values of 1.05 and 0.86.

There remains an important issue which we have not addressed so far. How much does the quality of the lattice data description improve as we increase the accuracy level of the chiral extrapolation formulae? In order to illustrate the significance of the N³LO approach we performed various fits to the lattice data at N²LO. A first chiral extrapolation study at the self consistent N²LO was reported in [18] prior to the availability of accurate lattice data. Like in Tab. III we perform fits to the data set where the maximum pion mass is restricted by a upper cutoff value. The parameters in Tab. IV correspond to an upper pion mass of 375 MeV and 475 MeV for the first two and the next two solutions respectively. All 9 parameters that are relevant at N²LO are listed in the table. Typically, for a given pion mass cutoff we

find two solutions of reasonable χ^2/N . The solutions labeled with Fit 375B and Fit 475B are characterized by axial coupling constants F and D that are significantly smaller than their known physical values. The solutions Fit 375A and Fit 475A have larger chi square values but predict values for F and D that are almost compatible with their empirical estimates. In order to further discriminate the two types of solutions we compute the baryon masses for the physical quark masses. While for the two A-type solutions the mean deviation from the empirical masses is about 10 MeV always, it is significantly larger for the two B-type solutions, for which the mean deviation is about 44 MeV in both cases. Note that all four solutions did not consider the physical baryon masses in their chi square definition. From this observation we conclude that in fact the A-type solutions are superior to the B-type solutions even though they describe the lattice data significantly worse. A further parameter set labeled by Fit A, given in the last column of IV, determined the low-energy parameters $\bar{b}_0, \bar{b}_D, \bar{b}_F$ and \bar{d}_0, \bar{d}_D from the physical baryon masses. In this case we use the empirical estimates $F = 0.45$ and $D = 0.80$ together with values for the parameters $\bar{M}_{[8]}$ and $\bar{M}_{[10]}$ from Fit 1 of Tab. I. This guarantees the fit to be compatible with our previous estimate of the baryon masses in their flavour SU(3) limit. The mean deviation of the baryon masses from their empirical values is also about 10 MeV in this case. Naturally, the quality of the lattice data description is worse here with $\chi^2/N \simeq 61.0$ and $\chi^2/N \simeq 40.2$ for the pion mass cut off at 375 MeV and 475 MeV respectively. Nevertheless, it is comforting to see that the values of the low-energy constants vary rather moderately from the solutions Fit 475A, Fit 375A to Fit A. The quality of the N³LO lattice data description in Tab. I is significantly improved as compared to the N²LO results of Tab. IV. This may justify the application of the chiral extrapolation at the self consistent N³LO as used throughout this work.

Based on the successful description of the currently available lattice data on the baryon masses we find it justified to generate detailed predictions for ongoing QCD lattice simulations of the ETM group. First results on the pion and nucleon mass for three distinct beta values are reported in [38] based on 2 +1 +1 simulations with twisted mass fermions. As a courtesy of C. Alexandrou we received the corresponding values of the kaon masses, with which we can attempt a prediction for their baryon octet and decuplet masses. In the first two columns of Tab. V we recall the lattice pion and kaon mass in units of the lattice scale. Like in our previous analysis we determine the optimal lattice scale for the three different

$a m_\pi$	$a m_K$	$a m_N$	$a m_\Lambda$	$a m_\Sigma$	$a m_\Xi$	$a m_\Delta$	$a m_{\Sigma^*}$	$a m_{\Xi^*}$	$a m_\Omega$
0.124,	0.252	0.511	0.577	0.607	0.654	0.662	0.718	0.772	0.825
0.149,	0.261	0.558	0.608	0.639	0.673	0.719	0.757	0.802	0.844
0.145,	0.259	0.539	0.595	0.624	0.664	0.693	0.739	0.787	0.834
0.141,	0.257	0.527	0.588	0.616	0.660	0.676	0.728	0.779	0.829
0.158,	0.262	0.544	0.600	0.626	0.667	0.692	0.739	0.786	0.832
0.173,	0.267	0.565	0.614	0.638	0.674	0.714	0.754	0.797	0.838
0.199,	0.277	0.592	0.635	0.654	0.687	0.736	0.772	0.809	0.845
0.223,	0.288	0.620	0.658	0.672	0.702	0.759	0.791	0.823	0.854
0.107,	0.212	0.455	0.506	0.530	0.569	0.593	0.636	0.679	0.720
0.126,	0.218	0.471	0.518	0.540	0.575	0.608	0.647	0.686	0.725
0.155,	0.228	0.500	0.539	0.557	0.586	0.632	0.664	0.698	0.730
0.180,	0.237	0.527	0.559	0.574	0.598	0.655	0.682	0.709	0.736
0.194,	0.244	0.549	0.577	0.588	0.610	0.676	0.699	0.723	0.746
0.070,	0.169	0.339	0.389	0.411	0.446	0.442	0.485	0.526	0.565
0.080,	0.173	0.347	0.394	0.416	0.451	0.450	0.491	0.530	0.569
0.098,	0.178	0.363	0.406	0.425	0.456	0.466	0.501	0.537	0.572
0.121,	0.176	0.391	0.418	0.433	0.453	0.495	0.517	0.541	0.564

TABLE V. Our prediction for the baryon octet and decuplet masses in units of the lattice scale a . The pion and kaon masses are taken from the ETM collaboration, where the first, second and third block in the table corresponds to β values of 1.90, 1.95 and 2.10 respectively. The uncertainty from taking either the parameters of Fit 1-4 is less than 0.002 in all cases.

beta values using our parameter sets. We find values

$$a_{\text{ETM}}^{\beta=1.90} \simeq 0.0980 \text{ fm}, \quad a_{\text{ETM}}^{\beta=1.95} \simeq 0.0880 \text{ fm}, \quad a_{\text{ETM}}^{\beta=2.10} \simeq 0.0674 \text{ fm}, \quad (33)$$

within the range obtained in [38]. Taking the lattice scales (33) we compute the nucleon mass

with respect to the ETM specifications and obtain with our Fit 1 parameters a $\chi^2/N \simeq 0.65$, $\chi^2/N \simeq 1.89$ and $\chi^2/N \simeq 0.29$ for the three beta values. Very similar values are obtained for all solutions of Tab. I and III, with the exception of solution B that leads to slightly worse chi square values of 1.13, 2.42 and 0.39 respectively. In the last eight columns of Tab. V we give our predictions for the baryon masses, where we take the average of the results obtained with our 4 different fit scenarios of Tab. I. The maximum deviation from our average is smaller or equal to 0.002 for all solutions of Tab. I. The spread is slightly larger if we consider also the solutions of III. Excluding the disfavored solution 245B the maximum uncertainty is 0.004. The Fit 245B leads to a slightly larger spread of 0.007.

PION AND STRANGENESS BARYON SIGMA TERMS

The pion- and strangeness baryon sigma terms are important parameters in various physical systems. They play a crucial role in dark matter searches (see e.g. [55, 56]). The strangeness sigma term is a key parameter for the determination of a possible kaon condensate in dense nuclear matter [57]. The pion-nucleon sigma term is of greatest relevance in the determination of the density dependence of the quark condensate at low baryon densities and therefore provides a first estimate of the critical baryon density at which chiral symmetry may be restored (see e.g. [48]).

Assuming exact isospin symmetry with $m_u = m_d \equiv m$, the pion-nucleon sigma term $\sigma_{\pi N}$ and the strangeness sigma term σ_{sN} are defined as follows

$$\sigma_{\pi N} = m \frac{\partial}{\partial m} m_N, \quad \sigma_{sN} = m_s \frac{\partial}{\partial m_s} m_N. \quad (34)$$

The sigma terms of the remaining baryon states are defined analogously to (34). In Tab. VI we present our predictions for the pion- and strangeness sigma terms of the baryon octet and decuplet states for our parameter sets of Tab. I.

In Tab. VI the sigma terms for the octet states are compared with two recent lattice determinations [6, 58]. Our values for the non-strange sigma terms are in reasonable agreement with the lattice results. In particular, we obtain a rather small value for the pion-nucleon sigma term $\sigma_{\pi N} = 39^{+2}_{-1}$ MeV, which is compatible with the seminal result $\sigma_{\pi N} = (45 \pm 8)$ MeV of Gasser, Leutwyler and Sainio in [59]. The size of the pion-nucleon term can be determined from the pion-nucleon scattering data. It requires a subtle subthreshold extrapolation of the scattering data [60]. Despite the long history of the sigma-term physics, the precise determination is still highly controversial (for one of the first reviews see e.g. [61]). Such a result is also consistent with the recent analysis of the QCDSF collaboration [62], which suggests a value $\sigma_{\pi N} = (38 \pm 12)$ MeV. In contrast there appears to be a slight tension with the recent analysis [63] that obtained $\sigma_{\pi N} = (52 \pm 3 \pm 8)$ MeV based on flavour SU(2) extrapolation of a large selection of lattice data for the nucleon mass.

In Tab. VI we include a first estimate of the uncertainties in the sigma terms from the different parameter sets in Tab. I and Tab. III. A full estimate of the systematic uncertainties is beyond the scope of this work. In particular, it would require a study of the corrections to the large- N_c sum rules our analysis relies on. For the counter terms required at N³LO such results are not available at present.

	[6]	[58]	[29]	Tab. 1	Error	Tab. 3	Error
$\sigma_{\pi N}$	$39(4)_{-7}^{+18}$	31(3)(4)	46(2)(12)	39.3	0.6	40.5	0.5
$\sigma_{\pi \Lambda}$	$29(3)_{-5}^{+11}$	24(3)(4)	20(2)(13)	23.1	0.3	23.4	0.5
$\sigma_{\pi \Sigma}$	$28(3)_{-3}^{+19}$	21(3)(3)	19(2)(6)	18.3	0.2	18.1	0.5
$\sigma_{\pi \Xi}$	$16(2)_{-3}^{+8}$	16(3)(4)	6(2)(5)	5.7	0.8	5.7	1.0
σ_{sN}	$34(14)_{-24}^{+28}$	71(34)(59)	157(25)(68)	84.2	3.3	100.8	11.7
$\sigma_{s\Lambda}$	$90(13)_{-38}^{+24}$	247(34)(69)	256(22)(60)	229.8	3.3	234.6	3.3
$\sigma_{s\Sigma}$	$122(15)_{-36}^{+25}$	336(34)(69)	270(22)(47)	355.2	4.6	358.9	6.2
$\sigma_{s\Xi}$	$156(16)_{-38}^{+36}$	468(35)(59)	369(23)(50)	368.2	8.0	362.9	13.3
	[21]	[26]	[30]	Tab. 1	Error	Tab. 3	Error
$\sigma_{\pi \Delta}$	55(4)(18)	34(3)	28(1)(8)	38.0	0.6	39.7	1.9
$\sigma_{\pi \Sigma^*}$	39(3)(13)	28(2)	22(2)(9)	26.8	0.6	27.2	0.9
$\sigma_{\pi \Xi^*}$	22(3)(7)	18(4)	11(2)(6)	13.7	0.5	14.0	0.9
$\sigma_{\pi \Omega}$	5(2)(1)	10(4)	5(2)(2)	4.4	0.9	5.0	0.9
$\sigma_{s\Delta}$	56(24)(1)	41(41)	88(22)(3)	42.5	3.8	63.6	26.5
$\sigma_{s\Sigma^*}$	160(28)(7)	211(44)	243(24)(31)	193.5	4.7	201.8	14.5
$\sigma_{s\Xi^*}$	274(32)(9)	373(53)	391(24)(67)	309.1	3.9	308.1	13.5
$\sigma_{s\Omega}$	360(34)(26)	510(50)	528(26)(101)	431.3	4.2	424.9	14.7

TABLE VI. Pion- and strangeness sigma terms of the baryon octet and decuplet states in units of MeV. A comparison with various theoretical predictions [6, 21, 26, 29, 30, 58] is provided. We take the average of sigma terms and strangeness contents as implied by the parameter sets of Tab. I and Tab. III separately. The associated errors identify the maximum deviation from the average within the given sample.

Our estimate for the strangeness sigma term of the nucleon with $\sigma_{sN} = 84_{-4}^{+28}$ MeV is significantly larger than the lattice average $\sigma_{sN} = 40_{-10}^{+10}$ MeV obtained in [64]. For the strangeness sigma terms of the remaining octet states there appears to be a striking conflict amongst the values obtained by the BMW and QCDSF-UKQCD groups. Our values are close to the values of the QCDSF-UKQCD group. The sigma terms for the baryon decuplet

states are compared with three previous extrapolation results [21, 26, 30]. Our values in Tab. VI are consistent with the previous analysis [26], based on the same framework used in this work. We observe that though the inclusion of finite volume effects is instrumental to determine the values of the symmetry preserving counter terms, the overall effect on the baryon decuplet masses at large volumes turns out rather small. There is also quite a consistency with the decuplet sigma terms obtained in [21, 30].

We close with a general comment on the convergence of a chiral expansion of the baryon masses. So far any strict chiral expansion without a partial summation of higher order terms did not lead to a satisfactory description of the lattice data. It is an interesting question how small the quark masses have to be chosen as to render the heavy-baryon framework meaningful in the flavour $SU(3)$ case. In principal given our parameter set we are in a position to identify the power counting regime as studied previously for the two flavour case in [65–67]. A detailed analysis of this issue is in preparation and will be provided elsewhere.

SUMMARY

In this work we reported on a comprehensive analysis of the available three flavour QCD lattice simulations of six different groups on the baryon octet and decuplet masses. We obtained an accurate 12 parameter description of altogether more than 220 lattice data points, where we kept all data with pion masses smaller than about 600 MeV. Our study is based on the relativistic three-flavour chiral Lagrangian with baryon octet and decuplet degrees of freedom. The baryon self energies were computed in a finite box at N³LO, where the physical masses are kept inside all loop integrals. The low-energy parameters were constrained by using large- N_c sum rules. In contrast to previous works all power-law finite volume corrections are incorporated for the decuplet baryons. We found their effects to be significant.

Predictions for all relevant low-energy parameters were obtained. In particular we extracted a pion-nucleon sigma term of 39^{+2}_{-1} MeV and a strangeness sigma term of the nucleon of $\sigma_{sN} = 84^{+28}_{-4}$ MeV. The flavour SU(3) chiral limit of the baryon octet and decuplet masses was determined with (802 ± 4) MeV and (1103 ± 6) MeV. In our fits we used the empirical masses of the baryon octet and decuplet states as a constraint. That allowed us to perform independent scale settings for the various lattice data. We obtained results for the lattice scales that are compatible with previous estimates, but appear to be much more accurate. Detailed predictions for the baryon masses as currently evaluated by the ETM lattice QCD group are made.

ACKNOWLEDGMENTS

Financial support from the Thailand Research Fund through the Royal Golden Jubilee Ph.D. Program (Grant No. PHD/0227/2553) to R. Bavontaweepanya and C. Kobdaj is acknowledged. C. Kobdaj was also partially supported by SUT research fund. M.F.M. Lutz thanks C. Alexandrou for providing a table with pion and kaon masses of an ongoing ETM simulation on the baryon masses and G. Schierholz for stimulating discussions on the QCDSF-UKQCD data. We are grateful to Rüdiger Berlich of Gemfony Scientific UG for help with the optimisation library Geneva.

APPENDIX A

We detail the running of the low-energy parameters on the renormalization scale μ , where we use the following convention

$$\bar{g} = \hat{g} - \frac{1}{4} \frac{\Gamma_g(\mu)}{(4\pi f)^2} \log \frac{\mu^2}{M^2}, \quad (\text{A.35})$$

with all parameters \hat{g} being scale independent. We find

$$\begin{aligned} \Gamma_{b_0} &= \frac{7 \Delta M (\Delta + 2M)^3}{72 (\Delta + M)^4} C^2, & \Gamma_{b_D} &= -\frac{\Delta M (\Delta + 2M)^3}{24 (\Delta + M)^4} C^2, \\ \Gamma_{b_F} &= \frac{5 \Delta M (\Delta + 2M)^3}{144 (\Delta + M)^4} C^2, & \Gamma_{d_0} &= -\frac{\Delta (\Delta + 2M)^3}{48 M^2 (\Delta + M)} C^2, \\ \Gamma_{d_D} &= -\frac{\Delta (\Delta + 2M)^3}{48 M^2 (\Delta + M)} C^2, \\ \\ \Gamma_{\zeta_0} &= -\frac{8 (13 D^2 + 9 F^2) (\Delta + M)^4 - 7 C^2 (\Delta + 2M)^2 (\Delta^2 + 4 \Delta M - 2 M^2)}{36 (\Delta + M)^4}, \\ \Gamma_{\zeta_D} &= \frac{12 (D^2 - 3 F^2) (\Delta + M)^4 - C^2 (\Delta + 2M)^2 (\Delta^2 + 4 \Delta M - 2 M^2)}{12 (\Delta + M)^4}, \\ \Gamma_{\zeta_F} &= -\frac{5 (48 D F (\Delta + M)^4 - C^2 (\Delta + 2M)^2 (\Delta^2 + 4 \Delta M - 2 M^2))}{72 (\Delta + M)^4}, \\ \Gamma_{\xi_0} &= -\frac{27 C^2 (4 M (\Delta + M)^3 + 3 (\Delta + M)^4 + M^4) + 200 H^2 M^2 (\Delta + M)^2}{648 M^2 (\Delta + M)^2}, \\ \Gamma_{\xi_D} &= -\frac{3 C^2 (4 M (\Delta + M)^3 + 3 (\Delta + M)^4 + M^4) + 40 H^2 M^2 (\Delta + M)^2}{72 M^2 (\Delta + M)^2}, \\ \\ \Gamma_{c_0} &= \frac{20 \bar{b}_0}{3} + 4 \bar{b}_D + 5 \frac{55 \gamma_C^{(0)} C^2 + 96 (D^2 + 3 F^2)}{432 M} \\ &\quad + \frac{1}{144} \left(-4 (30 g_0^{(S)} + 9 g_1^{(S)} + 26 g_D^{(S)}) - \bar{M}_{[8]} (30 g_0^{(V)} + 9 g_1^{(V)} + 26 g_D^{(V)}) \right) \\ &\quad - \frac{2}{27} \left(18 \hat{b}_D \left(\gamma_C^{(4)} C^2 + D^2 + 3 F^2 \right) + C^2 (15 \gamma_C^{(4)} \hat{b}_F - 11 \gamma_C^{(5)} \hat{d}_D) + 108 \hat{b}_F D F \right), \\ \Gamma_{c_1} &= \frac{96 (D^2 - 3 F^2) - 25 \gamma_C^{(0)} C^2}{216 M} + \frac{1}{24} \left(-4 g_1^{(S)} - g_1^{(V)} \bar{M}_{[8]} \right) \\ &\quad - \frac{4}{27} \left(6 \hat{b}_D \left(\gamma_C^{(4)} C^2 + 8 D^2 \right) + 5 C^2 (3 \gamma_C^{(4)} \hat{b}_F - \gamma_C^{(5)} \hat{d}_D) \right), \end{aligned}$$

$$\begin{aligned}
\Gamma_{c_2} &= \frac{2\bar{b}_D}{3} + \frac{25\gamma_C^{(0)}C^2 + 12D^2 - 36F^2}{36M} + \frac{1}{16} \left(4(g_1^{(S)} + g_D^{(S)}) + \bar{M}_{[8]}(g_1^{(V)} + g_D^{(V)}) \right) \\
&\quad + \frac{2}{9} \left(3\hat{b}_D \left(2\gamma_C^{(4)}C^2 + 5D^2 + 9F^2 \right) + C^2(15\gamma_C^{(4)}\hat{b}_F - 8\gamma_C^{(5)}\hat{d}_D) + 54\hat{b}_F D F \right), \\
\Gamma_{c_3} &= \frac{2\bar{b}_F}{3} - \frac{25\gamma_C^{(0)}C^2 + 96DF}{48M} + \frac{1}{16} \left(4g_F^{(S)} + g_F^{(V)}\bar{M}_{[8]} \right) \\
&\quad + \frac{2}{9} \left(5\hat{b}_D \left(\gamma_C^{(4)}C^2 + 6DF \right) + 3\hat{b}_F \left(-2\gamma_C^{(4)}C^2 + 5D^2 + 9F^2 \right) + 2C^2\gamma_C^{(5)}\hat{d}_D \right), \\
\Gamma_{c_4} &= \frac{44\bar{b}_D}{9} - 2\frac{25\gamma_C^{(0)}C^2 + 21(D^2 - 3F^2)}{27M} - \frac{1}{72} \left(36g_1^{(S)} + 52g_D^{(S)} + \bar{M}_{[8]}(9g_1^{(V)} + 13g_D^{(V)}) \right) \\
&\quad + \frac{4}{27} \left(-9\hat{b}_0\gamma_C^{(4)}C^2 + 3\hat{b}_D \left(\gamma_C^{(4)}C^2 + 8D^2 \right) + C^2(-15\gamma_C^{(4)}\hat{b}_F + 9\gamma_C^{(5)}\hat{d}_0 + 8\gamma_C^{(5)}\hat{d}_D) \right), \\
\Gamma_{c_5} &= \frac{44\bar{b}_F}{9} + 13\frac{25\gamma_C^{(0)}C^2 + 96DF}{216M} - \frac{13}{72} \left(4g_F^{(S)} + g_F^{(V)}\bar{M}_{[8]} \right) \\
&\quad + \frac{2}{27} C^2(15\gamma_C^{(4)}\hat{b}_0 + 42\gamma_C^{(4)}\hat{b}_F - 15\gamma_C^{(5)}\hat{d}_0 - 19\gamma_C^{(5)}\hat{d}_D), \\
\Gamma_{c_6} &= \frac{44\bar{b}_0}{9} + \frac{875\gamma_C^{(0)}C^2 + 896D^2 - 576F^2}{432M} \\
&\quad + \frac{1}{432} \left(-264g_0^{(S)} + 108g_1^{(S)} + 32g_D^{(S)} + \bar{M}_{[8]}(-66g_0^{(V)} + 27g_1^{(V)} + 8g_D^{(V)}) \right) \\
&\quad + \frac{2}{27} \left(42\hat{b}_0\gamma_C^{(4)}C^2 + 18\hat{b}_D \left(\gamma_C^{(4)}C^2 - 2D^2 \right) + C^2(15\gamma_C^{(4)}\hat{b}_F - 42\gamma_C^{(5)}\hat{d}_0 - 19\gamma_C^{(5)}\hat{d}_D) \right),
\end{aligned}$$

$$\begin{aligned}
\Gamma_{e_0} &= \frac{20\bar{d}_0}{3} + 2\bar{d}_D + \frac{81\gamma_C^{(1)}C^2 + 196\gamma_H^{(0)}H^2}{432M} \\
&\quad + \frac{1}{72} \left(-60\tilde{h}_1^{(S)} - 52\tilde{h}_2^{(S)} - 36\tilde{h}_3^{(S)} - \bar{M}_{[10]}(15h_1^{(V)} + 13h_2^{(V)} + 9h_3^{(V)}) \right) \\
&\quad + \frac{2}{3}C^2\gamma_C^{(2)}(\hat{b}_D - \hat{b}_F) - \frac{10\hat{d}_D H^2}{81}, \\
\Gamma_{e_1} &= \frac{27\gamma_C^{(1)}C^2 - 56\gamma_H^{(0)}H^2}{216M} + \frac{1}{12} \left(-4\tilde{h}_3^{(S)} - h_3^{(V)}\bar{M}_{[10]} \right) + \frac{4}{9}C^2(3\gamma_C^{(2)}\hat{b}_F - \gamma_C^{(3)}\hat{d}_D), \\
\Gamma_{e_2} &= \frac{2\bar{d}_D}{3} - \frac{27\gamma_C^{(1)}C^2 + 28\gamma_H^{(0)}H^2}{144M} + \frac{1}{8} \left(4(\tilde{h}_2^{(S)} + \tilde{h}_3^{(S)}) + \bar{M}_{[10]}(h_2^{(V)} + h_3^{(V)}) \right) \\
&\quad + \frac{2}{27} \left(-18C^2\gamma_C^{(2)}\hat{b}_D + 9C^2\gamma_C^{(3)}\hat{d}_D + 5\hat{d}_D H^2 \right), \\
\Gamma_{e_3} &= \frac{44\bar{d}_D}{9} + \frac{81\gamma_C^{(1)}C^2 + 196\gamma_H^{(0)}H^2}{216M} - \frac{1}{36} \left(52\tilde{h}_2^{(S)}36\tilde{h}_3^{(S)} + \bar{M}_{[10]}(13h_2^{(V)} + 9h_3^{(V)}) \right) \\
&\quad - \frac{2}{3}C^2(\gamma_C^{(2)}\hat{b}_0 + 2\gamma_C^{(2)}\hat{b}_F - \gamma_C^{(3)}\hat{d}_0 - \gamma_C^{(3)}\hat{d}_D), \\
\Gamma_{e_4} &= \frac{44\bar{d}_0}{9} - \frac{7\gamma_H^{(0)}H^2}{81M} + \frac{1}{216} \left(-132\tilde{h}_1^{(S)} + 16\tilde{h}_2^{(S)} - 33h_1^{(V)}\bar{M}_{[10]} + 4h_2^{(V)}\bar{M}_{[10]} \right)
\end{aligned}$$

$$-\frac{2}{3}C^2(\gamma_C^{(2)}\hat{b}_0 + \gamma_C^{(2)}\hat{b}_D - \gamma_C^{(2)}\hat{b}_F - \gamma_C^{(3)}\hat{d}_0), \quad (\text{A.36})$$

where all γ 's approach 1 in the limit $\Delta \rightarrow 0$. It holds

$$\begin{aligned} \gamma_C^{(0)} &= \frac{8\Delta^5 + 48\Delta^4 M + 120\Delta^3 M^2 + 156\Delta^2 M^3 + 102\Delta M^4 + 25M^5}{25(M+\Delta)^6} M, \\ \gamma_C^{(1)} &= \frac{(3M+\Delta)^2}{9M^3} (M-\Delta), \quad \gamma_C^{(2)} = \frac{(\Delta+2M)^2(\Delta^2+\Delta M+M^2)}{4M^3(\Delta+M)}, \\ \gamma_C^{(3)} &= \frac{(\Delta+2M)^2(3\Delta^2+4\Delta M+2M^2)}{8M^2(\Delta+M)^2}, \quad \gamma_C^{(5)} = \frac{(-\Delta+M)M^2(\Delta+2M)^2}{4(\Delta+M)^5}, \\ \gamma_C^{(4)} &= \frac{(-\Delta^2-4\Delta M+2M^2)(\Delta+2M)^2}{8(\Delta+M)^4}, \quad \gamma_H^{(0)} = \frac{M}{M+\Delta}, \end{aligned}$$

$$\tilde{h}_1^{(S)} = h_1^{(S)} + h_2^{(S)}/4, \quad \tilde{h}_2^{(S)} = h_3^{(S)} + h_4^{(S)}/4, \quad \tilde{h}_3^{(S)} = h_5^{(S)} + h_6^{(S)}/4. \quad (\text{A.37})$$

Note that the running of the symmetry breaking counter terms Γ_{c_i} and Γ_{e_i} includes the effect of the wave function factors Γ_ζ and Γ_ξ .

-
- [1] A. Walker-Loud *et al.*, Phys. Rev. **D79**, 054502 (2009), arXiv:0806.4549 [hep-lat].
 - [2] S. Aoki *et al.* (PACS-CS), Phys. Rev. **D79**, 034503 (2009), arXiv:0807.1661 [hep-lat].
 - [3] H.-W. Lin *et al.* (Hadron Spectrum), Phys. Rev. **D79**, 034502 (2009), arXiv:0810.3588 [hep-lat].
 - [4] S. Durr *et al.*, Science **322**, 1224 (2008), arXiv:0906.3599 [hep-lat].
 - [5] C. Alexandrou *et al.* (ETM Collaboration), Phys.Rev. **D80**, 114503 (2009), arXiv:0910.2419 [hep-lat].
 - [6] S. Durr *et al.*, Phys. Rev. **D85**, 014509 (2012), arXiv:1109.4265 [hep-lat].
 - [7] W. Bietenholz *et al.*, Phys.Rev. **D84**, 054509 (2011), arXiv:1102.5300 [hep-lat].
 - [8] A. Walker-Loud, Phys.Rev. **D86**, 074509 (2012), arXiv:1112.2658 [hep-lat].
 - [9] N. Kaiser, P. Siegel, and W. Weise, Nucl.Phys. **A594**, 325 (1995), arXiv:nucl-th/9505043 [nucl-th].
 - [10] M. F. M. Lutz and E. E. Kolomeitsev, Nucl. Phys. **A700**, 193 (2002), arXiv:nucl-th/0105042.
 - [11] Y. Ikeda, T. Hyodo, and W. Weise, Nucl.Phys. **A881**, 98 (2012), arXiv:1201.6549 [nucl-th].
 - [12] P. C. Bruns, M. Mai, and U. G. Meissner, Phys.Lett. **B697**, 254 (2011), arXiv:1012.2233 [nucl-th].

- [13] E. Jenkins and A. V. Manohar, Phys. Lett. B **255**, 558 (1991).
- [14] A. Walker-Loud, Nucl.Phys. **A747**, 476 (2005), arXiv:hep-lat/0405007 [hep-lat].
- [15] B. C. Tiburzi and A. Walker-Loud, Nucl.Phys. **A748**, 513 (2005), arXiv:hep-lat/0407030 [hep-lat].
- [16] A. Semke and M. F. M. Lutz, Nucl. Phys. **A778**, 153 (2006), arXiv:nucl-th/0511061.
- [17] M. Frink and U.-G. Meissner, Eur. Phys. J. **A29**, 255 (2006), arXiv:hep-ph/0609256.
- [18] A. Semke and M. F. M. Lutz, Nucl. Phys. **A789**, 251 (2007).
- [19] B. C. Tiburzi and A. Walker-Loud, Phys.Lett. **B669**, 246 (2008), arXiv:0808.0482 [nucl-th].
- [20] F.-J. Jiang, B. C. Tiburzi, and A. Walker-Loud, Phys.Lett. **B695**, 329 (2011), arXiv:0911.4721 [nucl-th].
- [21] J. Martin Camalich, L. S. Geng, and M. J. Vicente Vacas, Phys. Rev. **D82**, 074504 (2010), arXiv:1003.1929 [hep-lat].
- [22] R. D. Young and A. W. Thomas, Phys. Rev. D **81**, 014503 (2010).
- [23] L.-s. Geng, X.-l. Ren, J. Martin-Camalich, and W. Weise, Phys.Rev. **D84**, 074024 (2011), arXiv:1108.2231 [hep-ph].
- [24] J. Martin Camalich, L. Geng, and M. Vicente Vacas, AIP Conf.Proc. **1322**, 440 (2010).
- [25] A. Semke and M. F. M. Lutz, Phys.Rev. **D85**, 034001 (2012), arXiv:1111.0238 [hep-ph].
- [26] A. Semke and M. F. M. Lutz, Phys.Lett. **B717**, 242 (2012), arXiv:1202.3556 [hep-ph].
- [27] M. F. M. Lutz and A. Semke, Phys.Rev. **D86**, 091502 (2012), arXiv:1209.2791 [hep-lat].
- [28] P. Bruns, L. Greil, and A. Schafer, (2012), arXiv:1209.0980 [hep-ph].
- [29] X.-L. Ren, L. Geng, J. Meng, and H. Toki, Phys.Rev. **D87**, 074001 (2013), arXiv:1302.1953 [nucl-th].
- [30] X.-L. Ren, L.-S. Geng, and J. Meng, (2013), arXiv:1307.1896.
- [31] J. Gegelia and G. Japaridze, Phys.Rev. **D60**, 114038 (1999), arXiv:hep-ph/9908377 [hep-ph].
- [32] T. Becher and H. Leutwyler, Eur.Phys.J. **C9**, 643 (1999), arXiv:hep-ph/9901384 [hep-ph].
- [33] X.-L. Ren, L. Geng, J. Martin Camalich, J. Meng, and H. Toki, JHEP **1212**, 073 (2012), arXiv:1209.3641 [nucl-th].
- [34] V. Pascalutsa, Phys.Rev. **D58**, 096002 (1998), arXiv:hep-ph/9802288 [hep-ph].
- [35] V. Pascalutsa and R. Timmermans, Phys.Rev. **C60**, 042201 (1999), arXiv:nucl-th/9905065 [nucl-th].
- [36] M. F. M. Lutz and A. Semke, Phys. Rev. **D83**, 034008 (2011), arXiv:1012.4365 [hep-ph].

- [37] E. E. Jenkins, A. V. Manohar, J. W. Negele, and A. Walker-Loud, Phys.Rev. **D81**, 014502 (2010), arXiv:0907.0529 [hep-lat].
- [38] C. Alexandrou, M. Constantinou, S. Dinter, V. Drach, K. Jansen, *et al.*, Phys.Rev. **D88**, 014509 (2013), arXiv:1303.5979 [hep-lat].
- [39] X.-L. Ren, L.-S. Geng, and J. Meng, (2013), arXiv:1311.7234 [hep-ph].
- [40] J. Gasser and H. Leutwyler, Nucl. Phys. **B250**, 465 (1985).
- [41] P. Hasenfratz and H. Leutwyler, Nucl.Phys. **B343**, 241 (1990).
- [42] J. Bijnens and I. Jemos, Nucl.Phys. **B854**, 631 (2012), arXiv:1103.5945 [hep-ph].
- [43] E. E. Jenkins and R. F. Lebed, Phys. Rev. **D52**, 282 (1995), hep-ph/9502227.
- [44] M. Luscher, Commun.Math.Phys. **105**, 153 (1986).
- [45] G. Bali, P. Bruns, S. Collins, M. Deka, B. Glasle, *et al.*, Nucl.Phys. **B866**, 1 (2013), arXiv:1206.7034 [hep-lat].
- [46] L. Leskovec and S. Prelovsek, Phys.Rev. **D85**, 114507 (2012), arXiv:1202.2145 [hep-lat].
- [47] G. Passarino and M. Veltman, Nucl.Phys. **B160**, 151 (1979).
- [48] M. F. M. Lutz, B. Friman, and C. Appel, Phys. Lett. **B474**, 7 (2000), arXiv:nucl-th/9907078.
- [49] R. F. Dashen, E. E. Jenkins, and A. V. Manohar, Phys. Rev. **D49**, 4713 (1994), hep-ph/9310379.
- [50] M. F. M. Lutz and E. E. Kolomeitsev, Nucl. Phys. **A700**, 193 (2002).
- [51] A. Walker-Loud, PoS **LATTICE2008**, 005 (2008), arXiv:0810.0663 [hep-lat].
- [52] A. Walker-Loud, PoS **CD12**, 017 (2013), arXiv:1304.6341 [hep-lat].
- [53] M. F. M. Lutz and A. Semke, PoS **CD12**, 074 (2013), arXiv:1301.0298.
- [54] A. Walker-Loud, H.-W. Lin, D. Richards, R. Edwards, M. Engelhardt, *et al.*, Phys.Rev. **D79**, 054502 (2009), arXiv:0806.4549 [hep-lat].
- [55] G. Belanger, F. Boudjema, A. Pukhov, and A. Semenov, (2013), arXiv:1305.0237 [hep-ph].
- [56] A. Crivellin, M. Hoferichter, and M. Procura, (2013), arXiv:1312.4951 [hep-ph].
- [57] D. Kaplan and A. Nelson, Phys.Lett. **B175**, 57 (1986).
- [58] R. Horsley *et al.*, arXiv:1110.4971 [hep-lat] (2011), arXiv:1110.4971 [hep-lat].
- [59] J. Gasser, H. Leutwyler, and M. Sainio, Phys.Lett. **B253**, 252 (1991).
- [60] C. Ditsche, M. Hoferichter, B. Kubis, and U.-G. Meissner, PoS **CD12**, 064 (2013), arXiv:1211.7285 [hep-ph].
- [61] E. Reya, Rev. Mod. Phys. **46**, 545 (1974).

- [62] G. S. Bali *et al.* (QCDSF), arXiv:1111.1600 [hep-lat] (2011), arXiv:1111.1600 [hep-lat].
- [63] L. Alvarez-Ruso, T. Ledwig, J. Martin Camalich, and M. Vicente-Vacas, Phys.Rev. **D88**, 054507 (2013), arXiv:1304.0483 [hep-ph].
- [64] P. Junnarkar and A. Walker-Loud, Phys.Rev. **D87**, 114510 (2013), arXiv:1301.1114 [hep-lat].
- [65] R. D. Young, D. B. Leinweber, and A. W. Thomas, Prog.Part.Nucl.Phys. **50**, 399 (2003), arXiv:hep-lat/0212031 [hep-lat].
- [66] D. B. Leinweber, A. W. Thomas, and R. D. Young, Phys.Rev.Lett. **92**, 242002 (2004), arXiv:hep-lat/0302020 [hep-lat].
- [67] D. B. Leinweber, A. W. Thomas, and R. D. Young, Nucl.Phys. **A755**, 59 (2005), arXiv:hep-lat/0501028 [hep-lat].